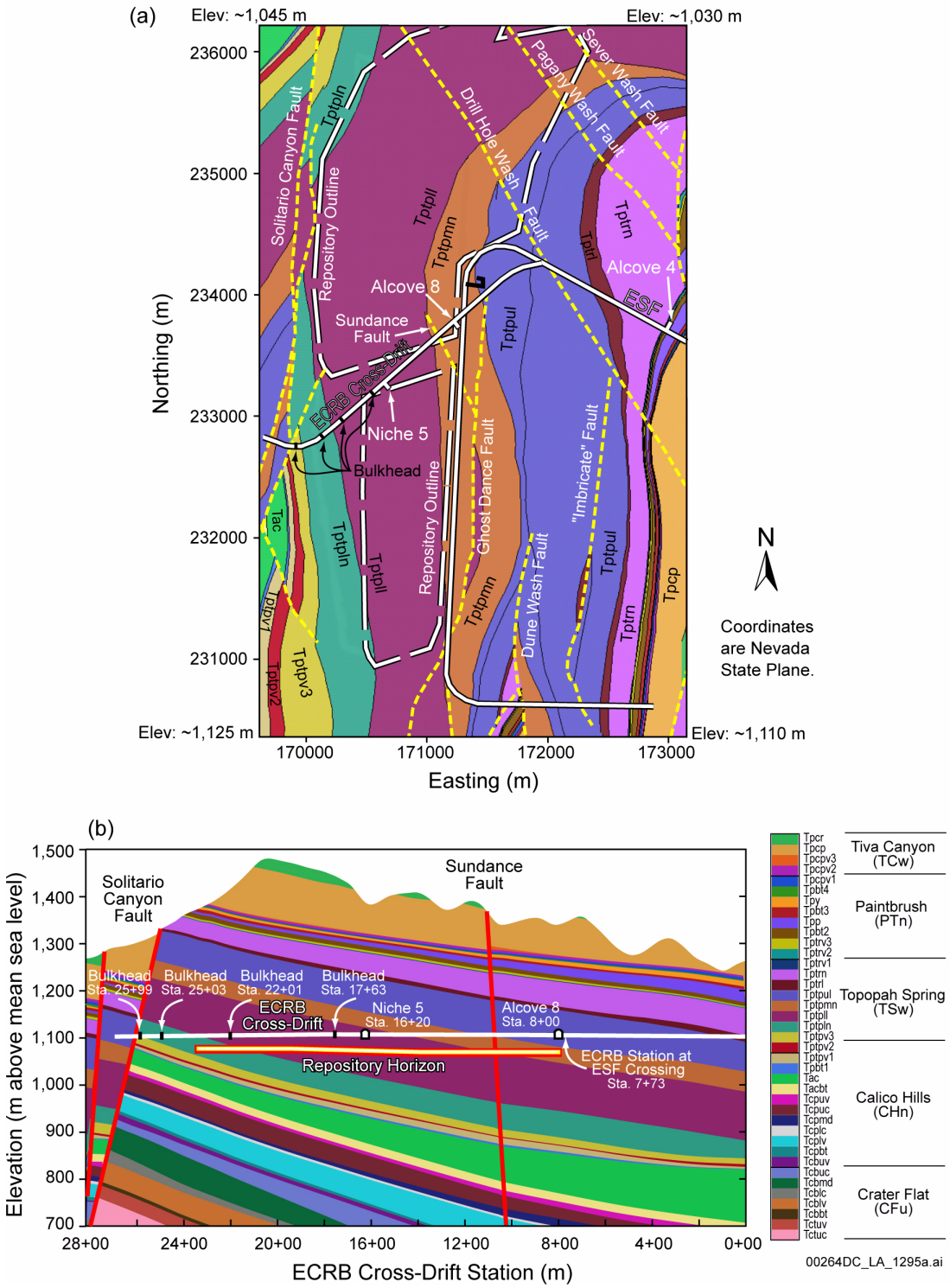

Figure 2.3.2-9. Lithostratigraphic Units and Major Hydrogeologic Units of Yucca Mountain in (a) Plan View through the Repository Horizon and (b) Vertical Cross Section Along the ECRB Cross-Drift

Source: BSC 2004i, Figure 1-1.

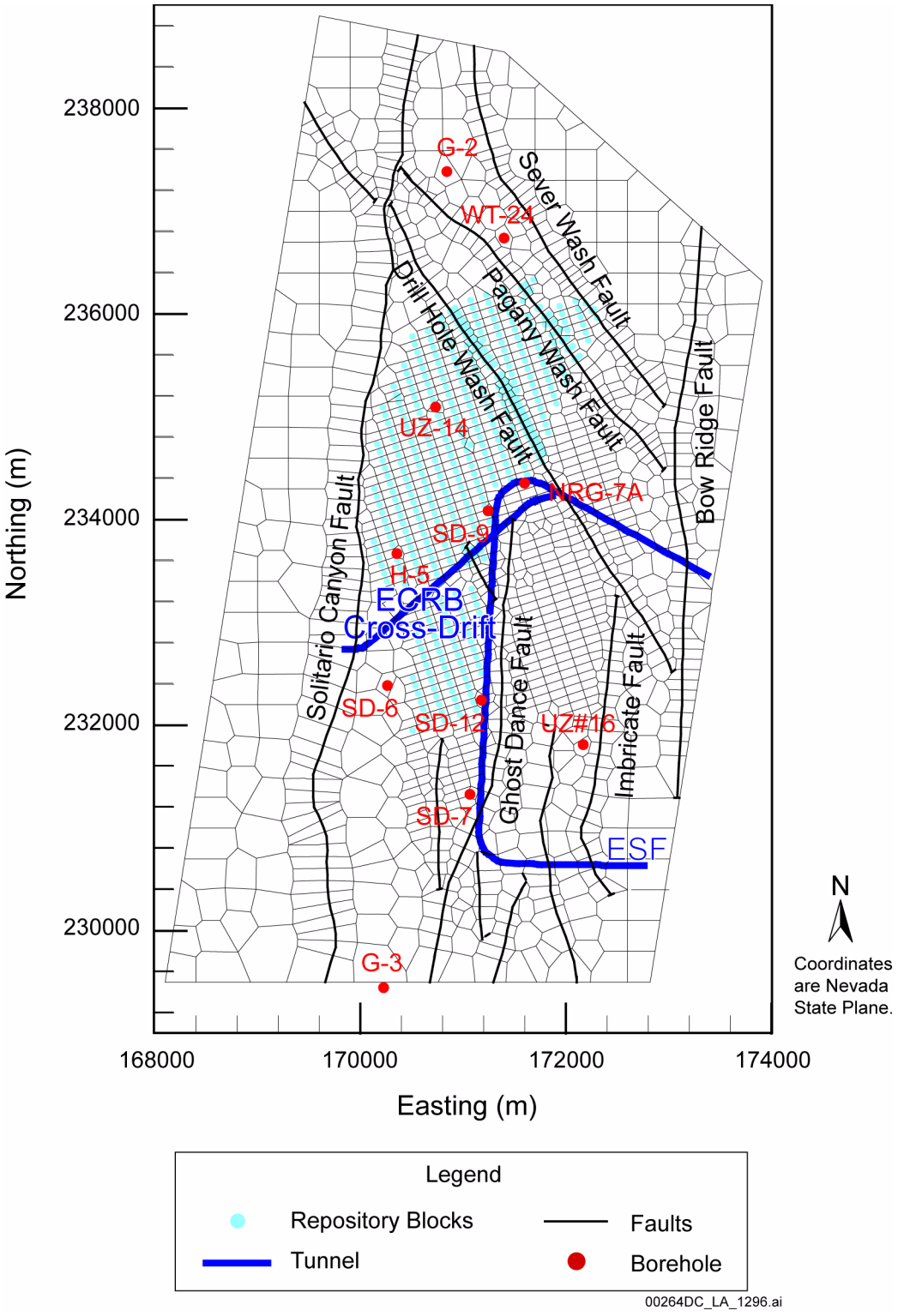

Figure 2.3.2-10. Plan View of the Three-Dimensional Site-Scale Unsaturated Zone Flow Model Domain

Source: SNL 2007a, Figure 6.1-1.

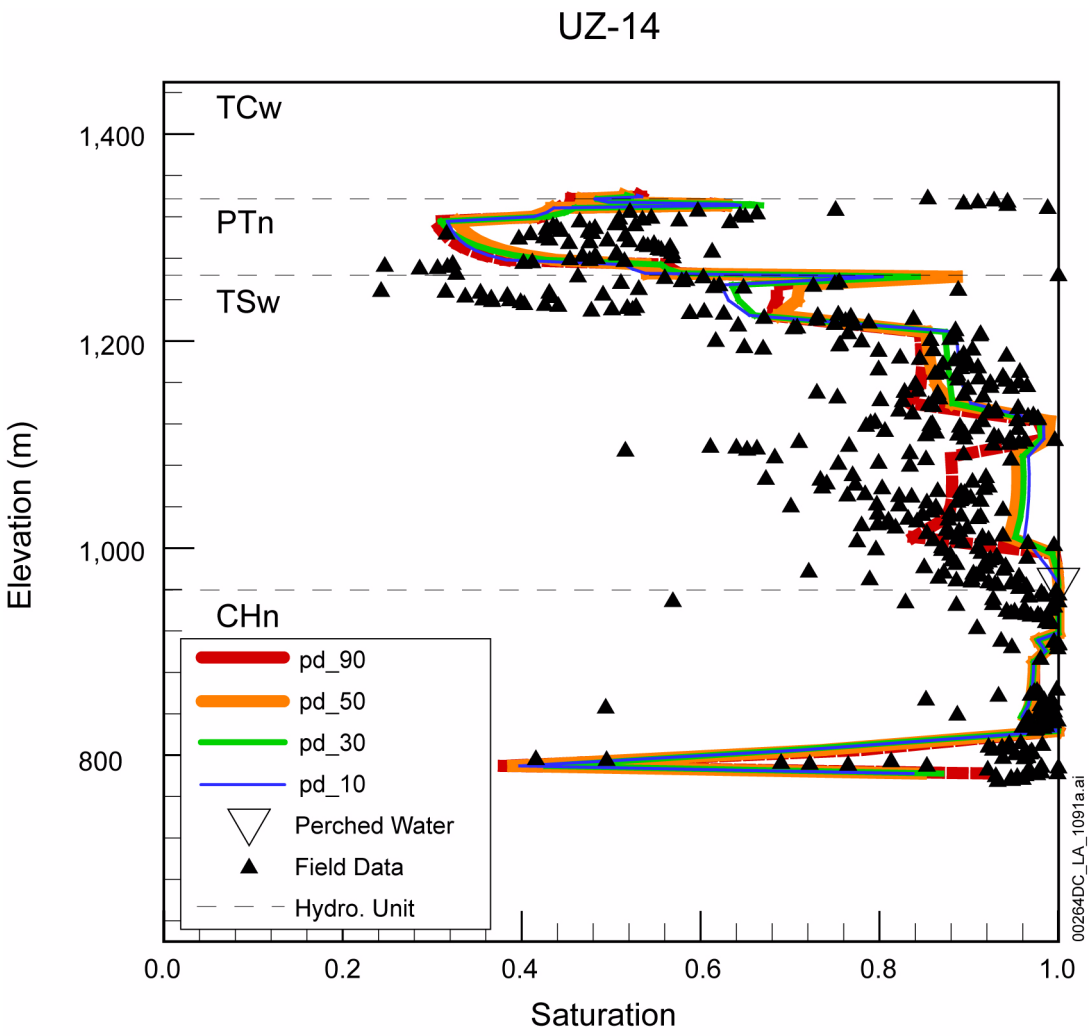

Figure 2.3.2-11. Comparison of the Simulated to the Observed Matrix Liquid Saturations and Perched-Water Elevations for Borehole USW UZ-14, Using the Results of the Simulations with Four Present-Day (pd) Infiltration Rates

Source: SNL 2007a, Figure 6.2-2.

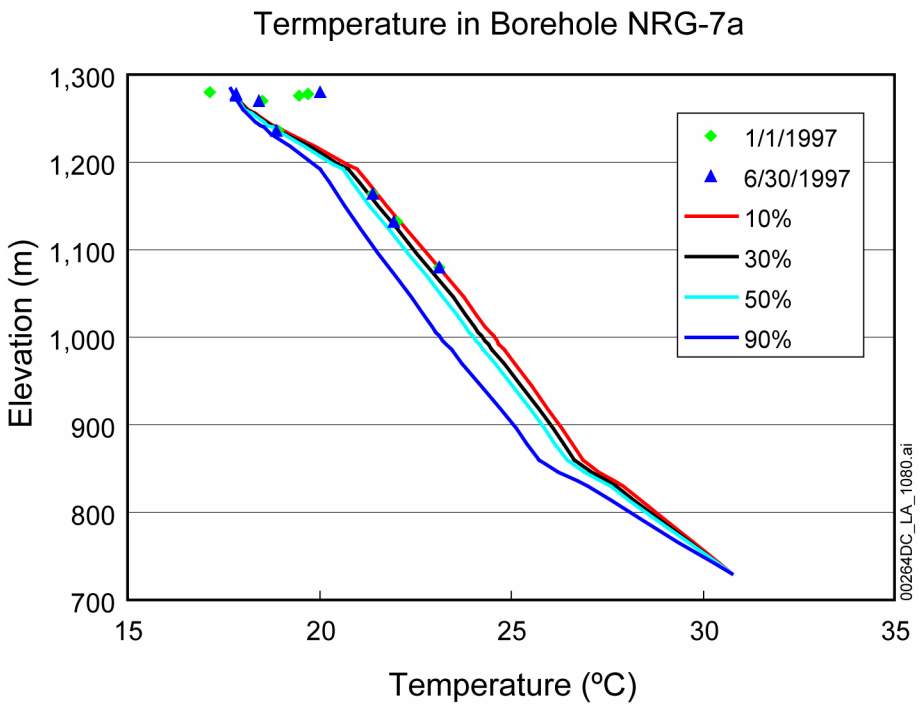

Figure 2.3.2-12. Comparisons between Measured and Modeled Ambient Temperature Profiles in Borehole NRG-7A for the Four Infiltration Maps of 10th, 30th, 50th and 90th Percentile Present-Day Infiltration Rates

Source: SNL 2007a, Figure 6.3-3.

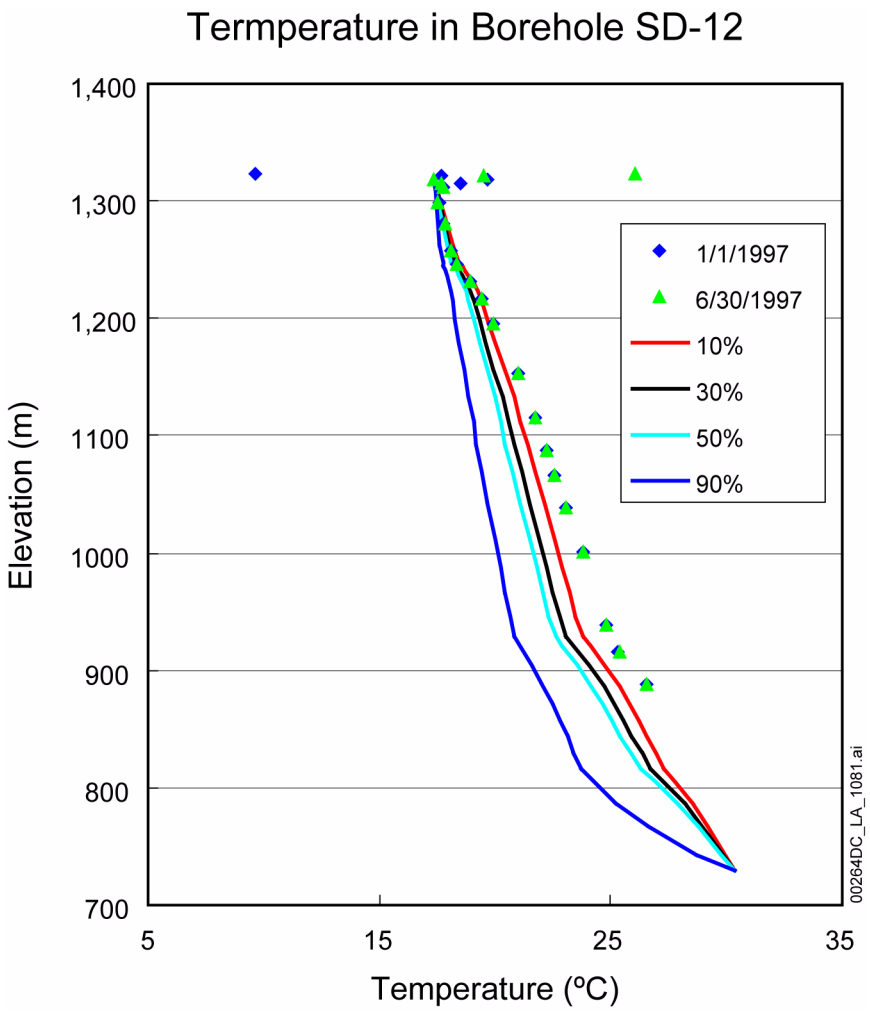

Figure 2.3.2-13. Comparisons between Measured and Modeled Ambient Temperature Profiles in Borehole SD-12 for the Four Infiltration Maps of 10th, 30th, 50th and 90th Percentile Present-Day Infiltration Rates

Source: SNL 2007a, Figure 6.3-4.

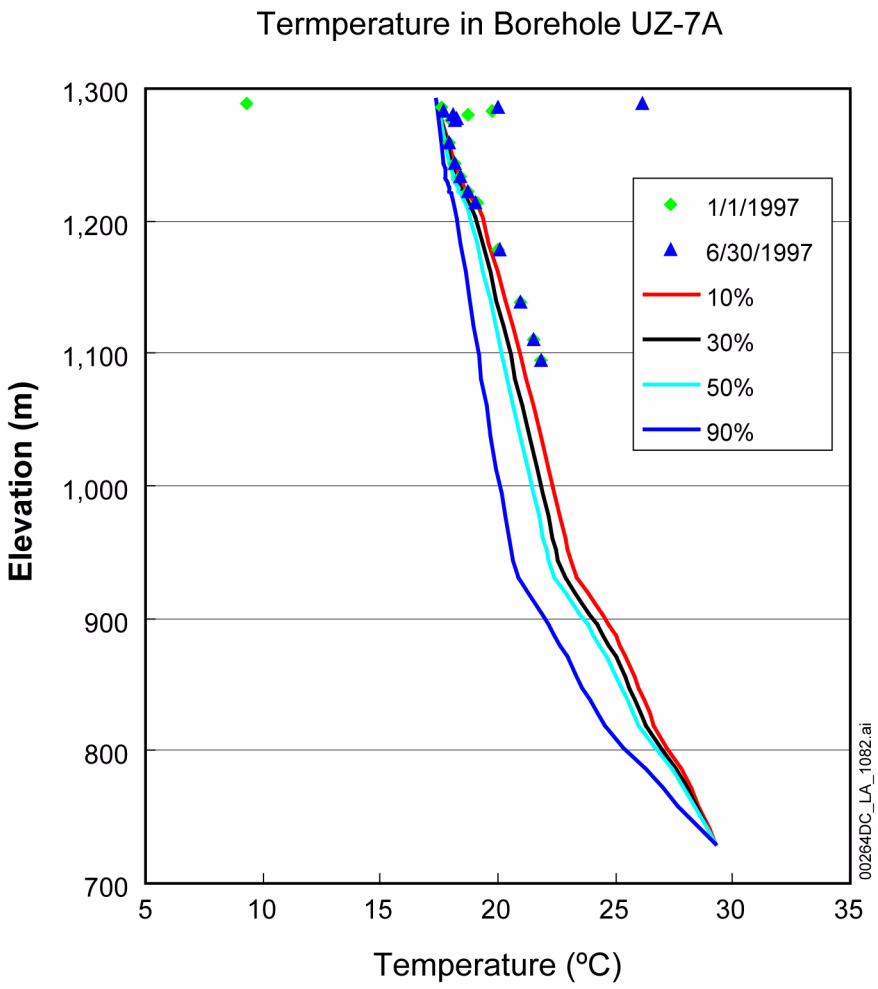

Figure 2.3.2-14. Comparisons between Measured and Modeled Ambient Temperature Profiles in Borehole UZ-7a for the Four Infiltration Maps of 10th, 30th, 50th and 90th Percentile Present-Day Infiltration Rates

Source: SNL 2007a, Figure 6.3-5.

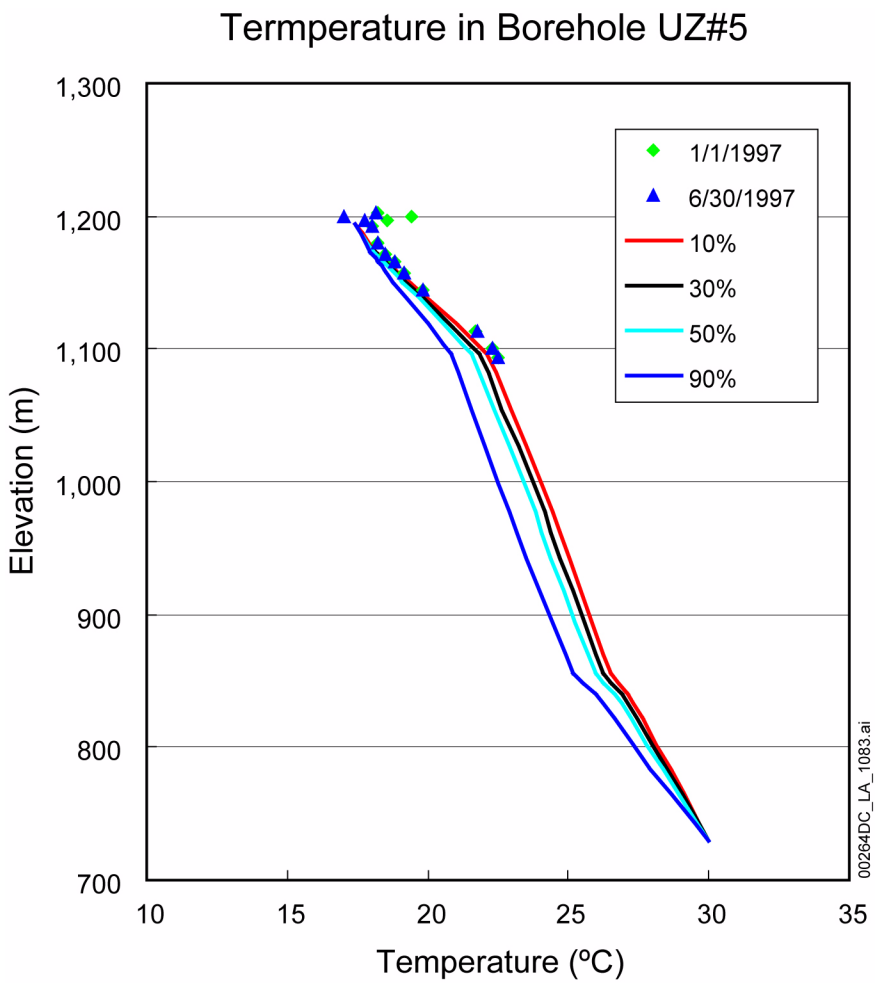

Figure 2.3.2-15. Comparisons between Measured and Modeled Ambient Temperature Profiles in Borehole UZ#5 for the Four Infiltration Maps of 10th, 30th, 50th and 90th Percentile Present-Day Mean Infiltration Rates

Source: SNL 2007a, Figure 6.3-6.

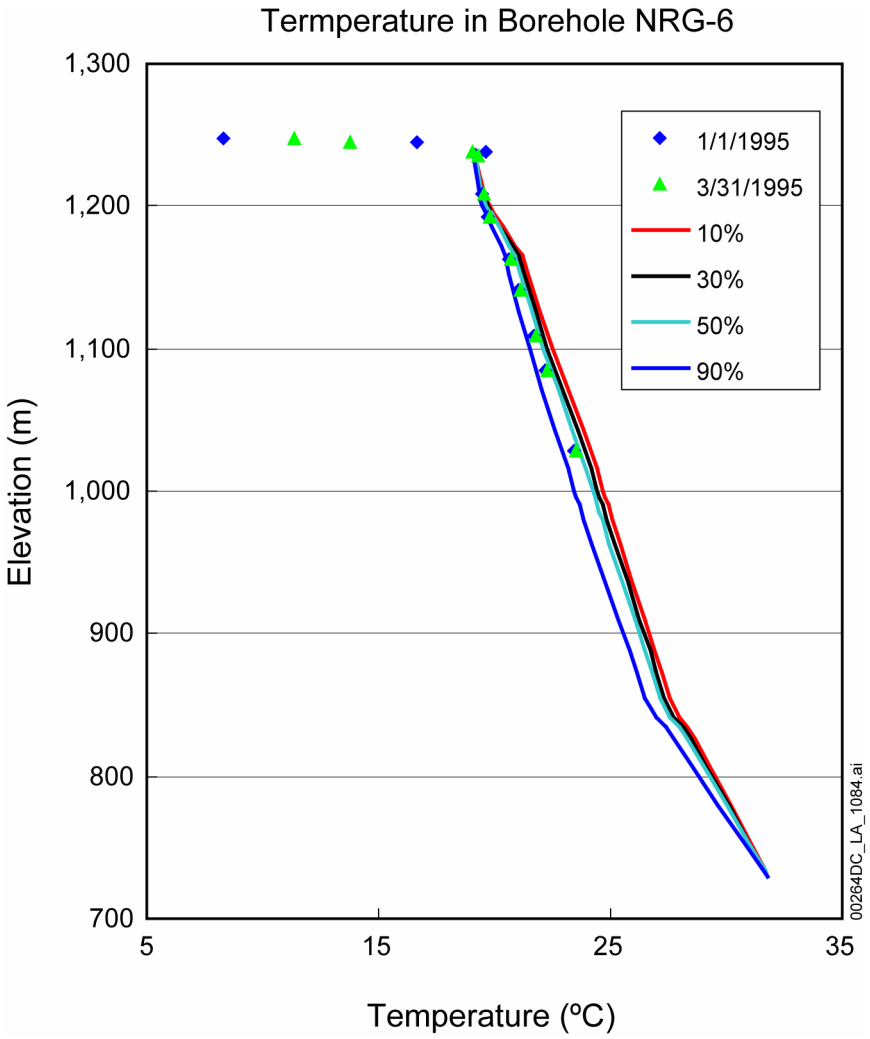

Figure 2.3.2-16. Comparisons between Measured and Modeled Ambient Temperature Profiles in Borehole NRG-6 for the Four Infiltration Maps of 10th, 30th, 50th and 90th Percentile Present-Day Infiltration Rates

Source: SNL 2007a, Figure 6.3-2.

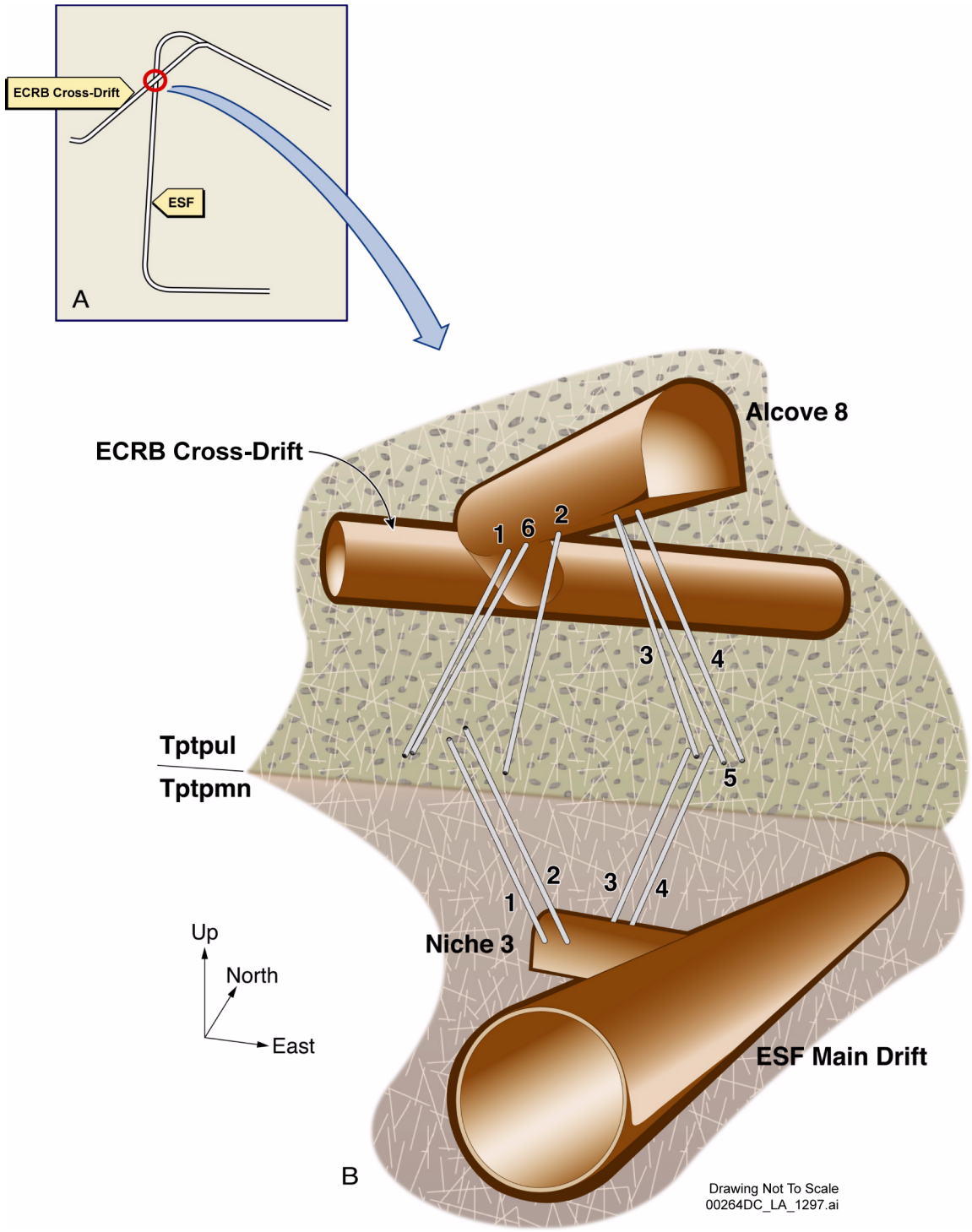

Figure 2.3.2-17. Location of Test Bed between the Enhanced Characterization of the Repository Block Cross-Drift and Exploratory Studies Facility Main Drift

Source: BSC 2004i, Figure 6-149.

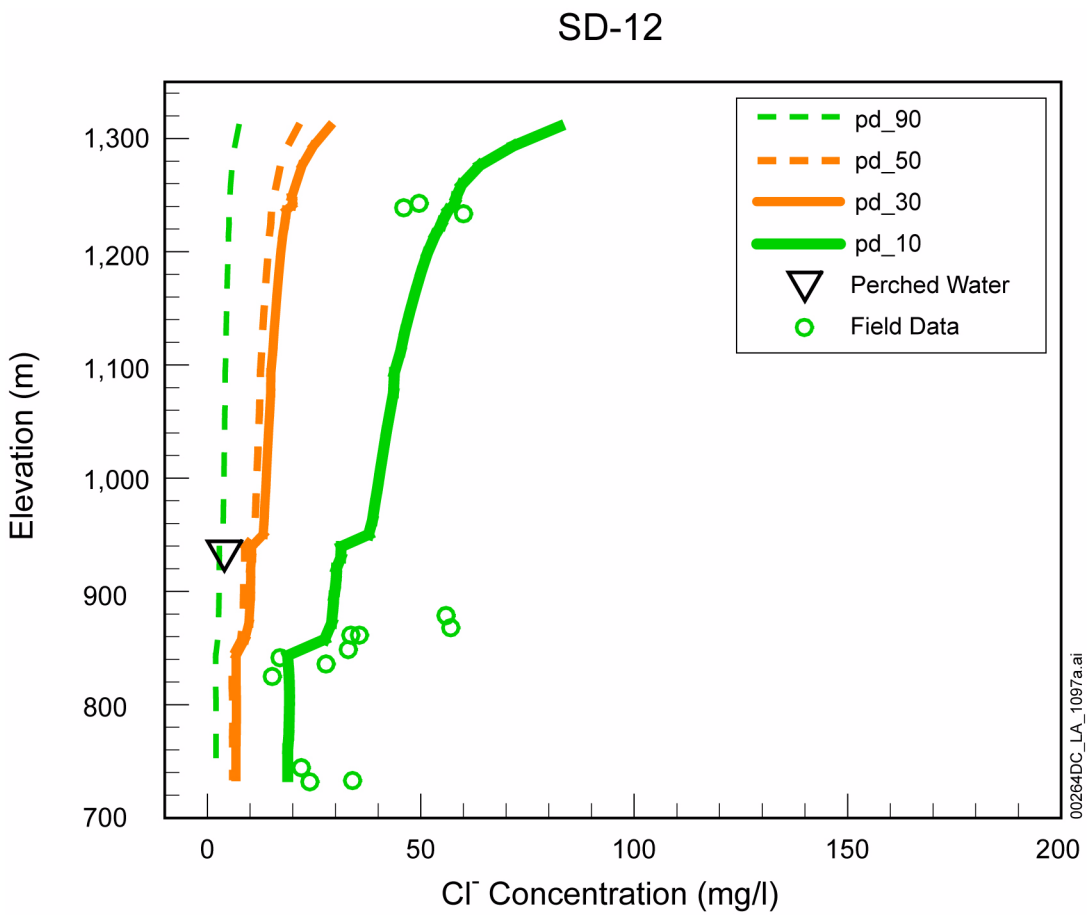

Figure 2.3.2-18. Chloride Concentration (mg/L) Profiles at Borehole USW SD-12 for Present-Day 10th, 30th, 50th, and 90th Percentile Infiltration Maps

Source: SNL 2007a, Figure 6.5-1.

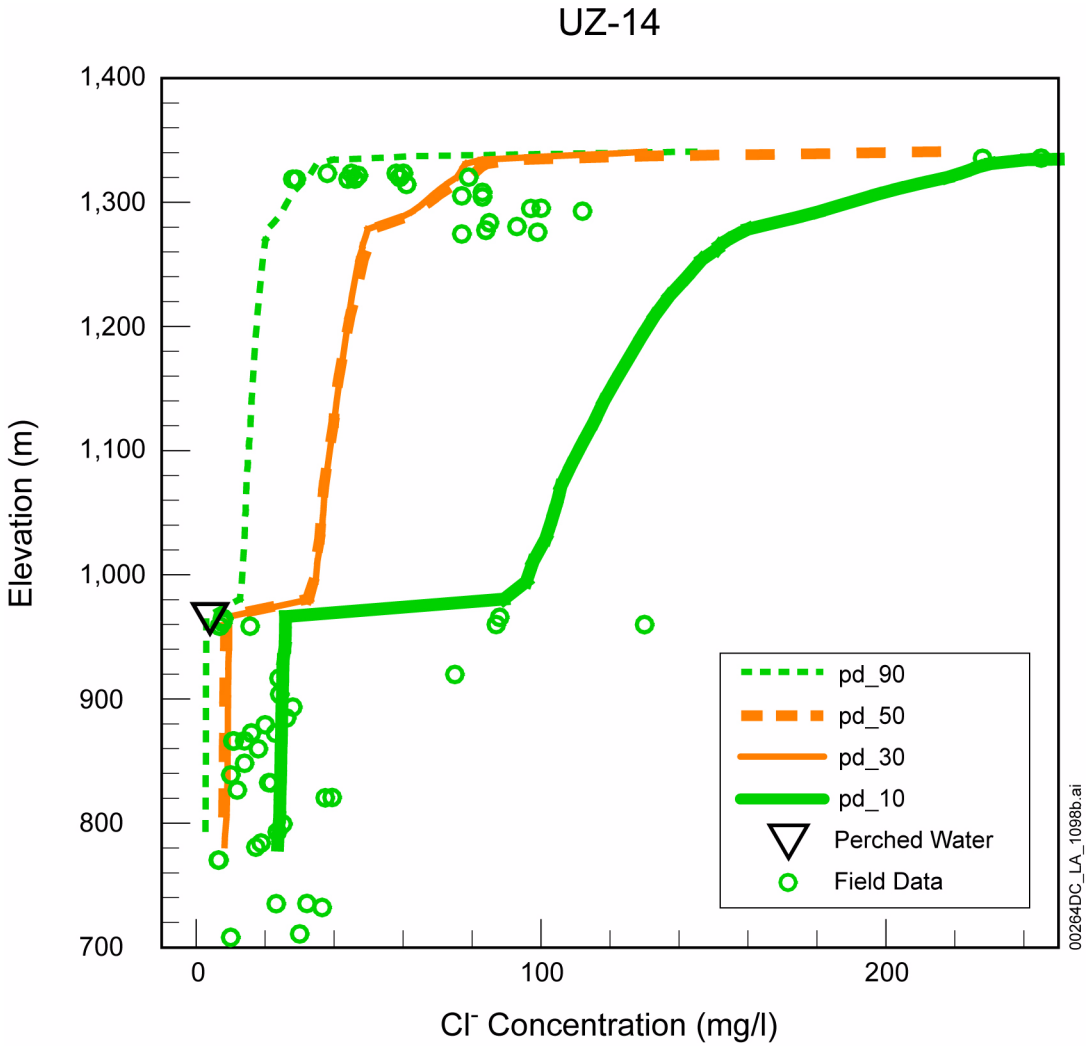

Figure 2.3.2-19. Chloride Concentration (mg/L) Profiles at Borehole USW UZ-14 for Present-Day 10th, 30th, 50th, and 90th Percentile Infiltration Maps

Source: SNL 2007a, Figure 6.5-2.

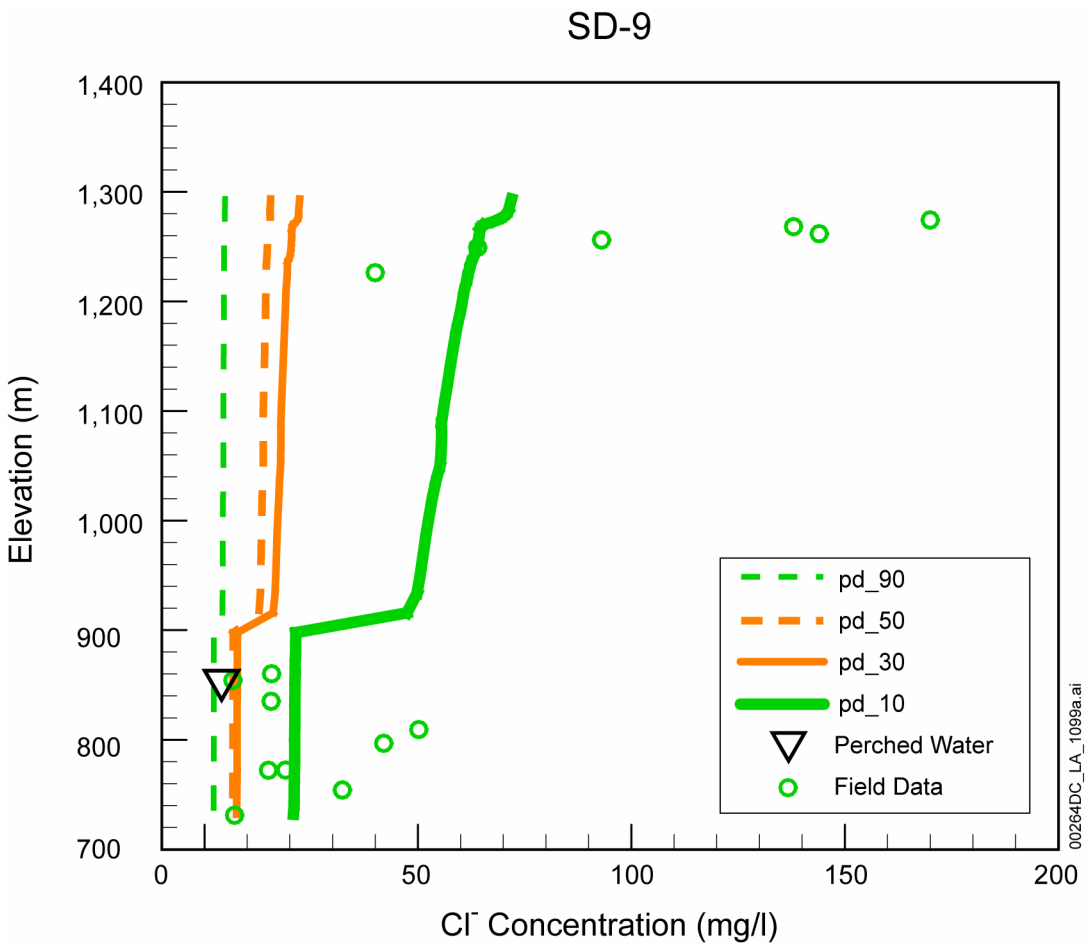

Figure 2.3.2-20. Chloride Concentration (mg/L) Profiles at Borehole USW SD-9 for Present-Day 10th, 30th, 50th, and 90th Percentile Infiltration Maps

Source: SNL 2007a, Figure 6.5-3.

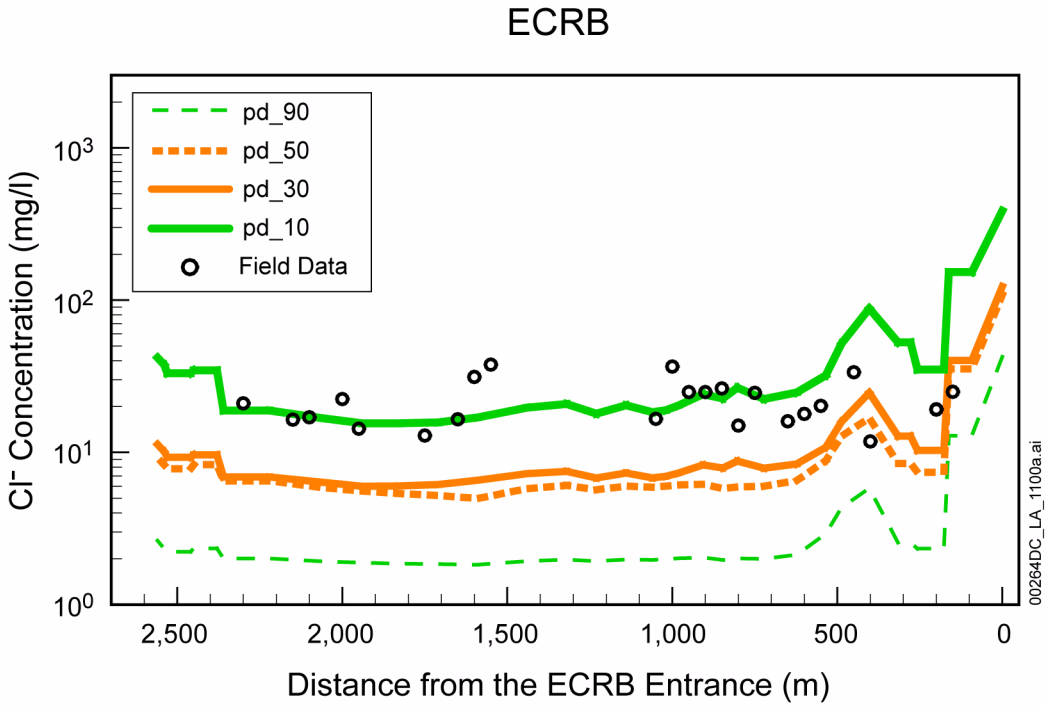

Figure 2.3.2-21. Chloride Concentration (mg/L) Profiles at the ECRB Cross-Drift for Present-Day 10th, 30th, 50th, and 90th Percentile Infiltration Maps

Source: SNL 2007a, Figure 6.5-4.

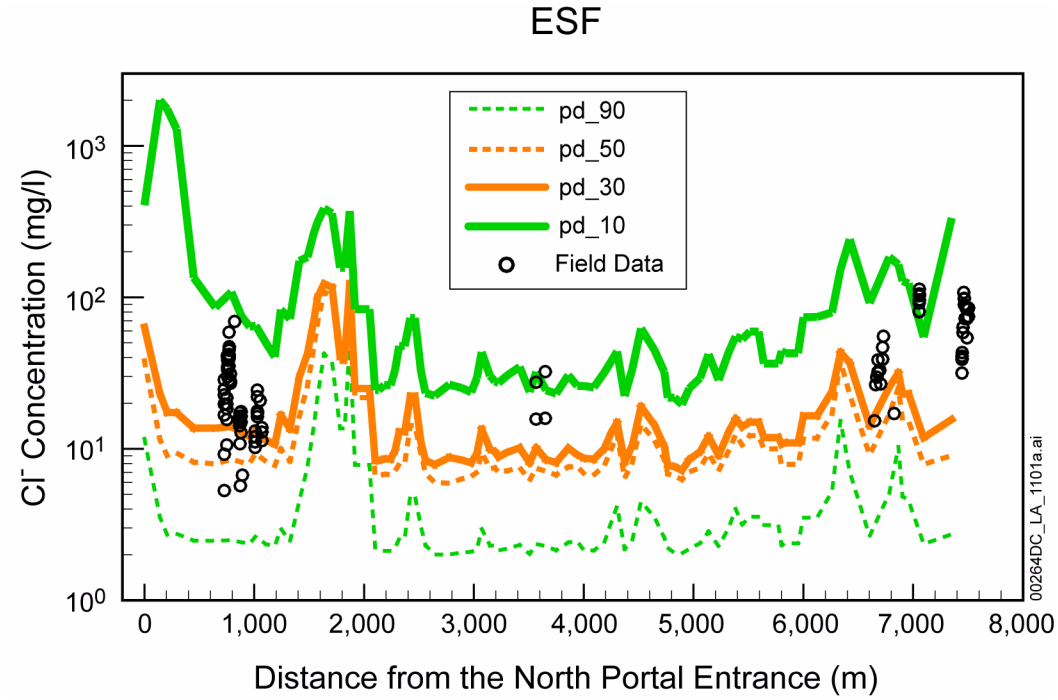

Figure 2.3.2-22. Chloride Concentration (mg/L) Profiles at the ESF for Present-Day 10th, 30th, 50th, and 90th Percentile Infiltration Maps

Source: SNL 2007a, Figure 6.5-5.

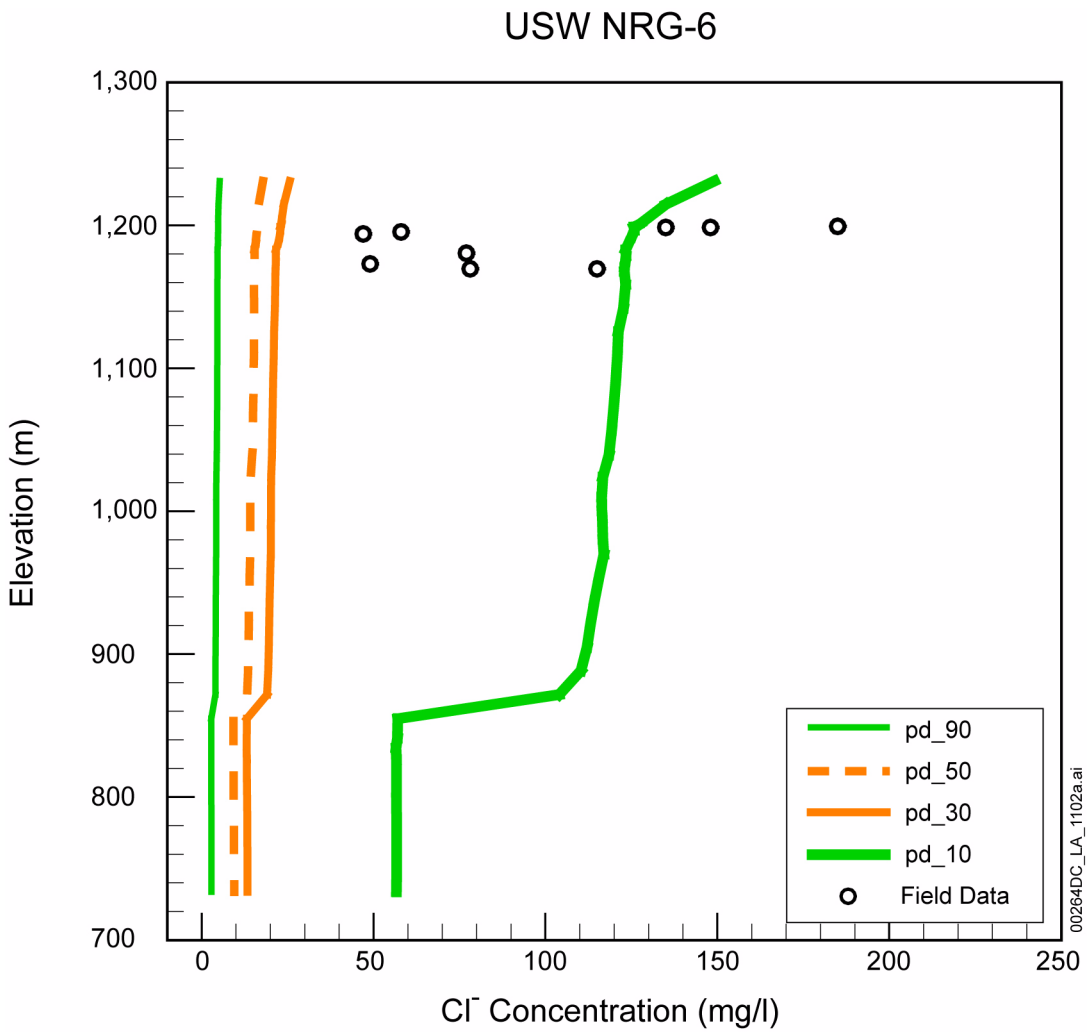

Figure 2.3.2-23. Chloride Concentration (mg/L) Profiles at Borehole USW NRG-6 for Present-Day 10th, 30th, 50th, and 90th Percentile Infiltration Maps

Source: SNL 2007a, Figure 6.5-6.

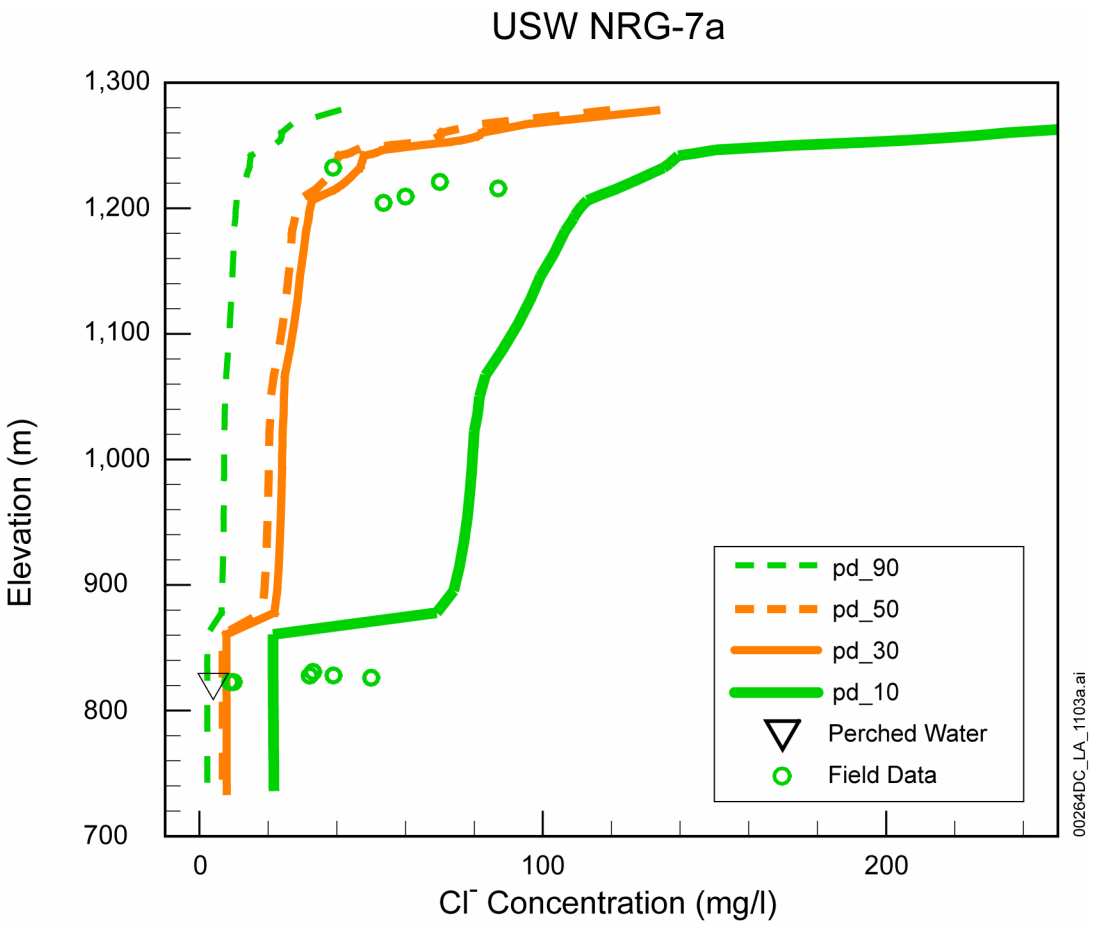

Figure 2.3.2-24. Chloride Concentration (mg/L) Profiles at Borehole USW NRG-7a for Present-Day 10th, 30th, 50th, and 90th Percentile Infiltration Maps

Source: SNL 2007a, Figure 6.5-7.

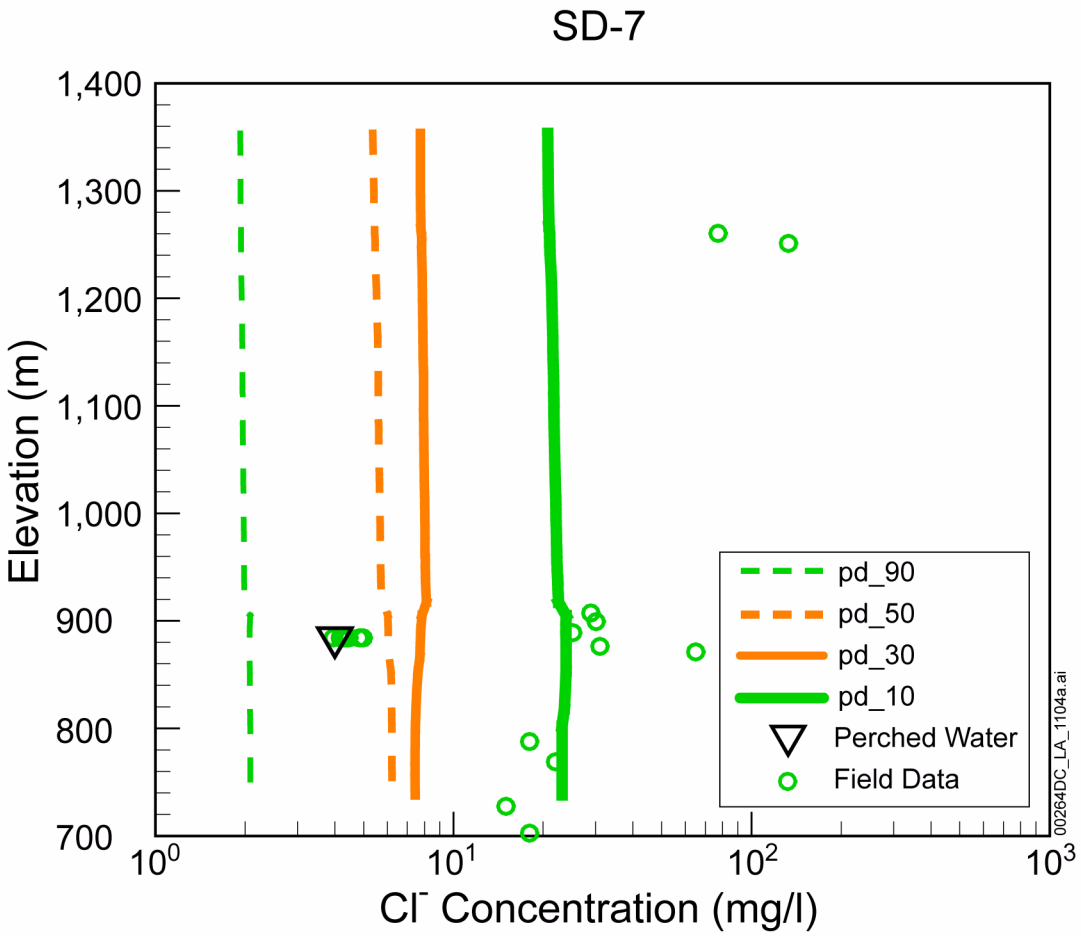

Figure 2.3.2-25. Chloride Concentration (mg/L) Profiles at Borehole USW SD-7 for Present-Day 10th, 30th, 50th, and 90th Percentile Infiltration Maps

Source: SNL 2007a, Figure 6.5-8.

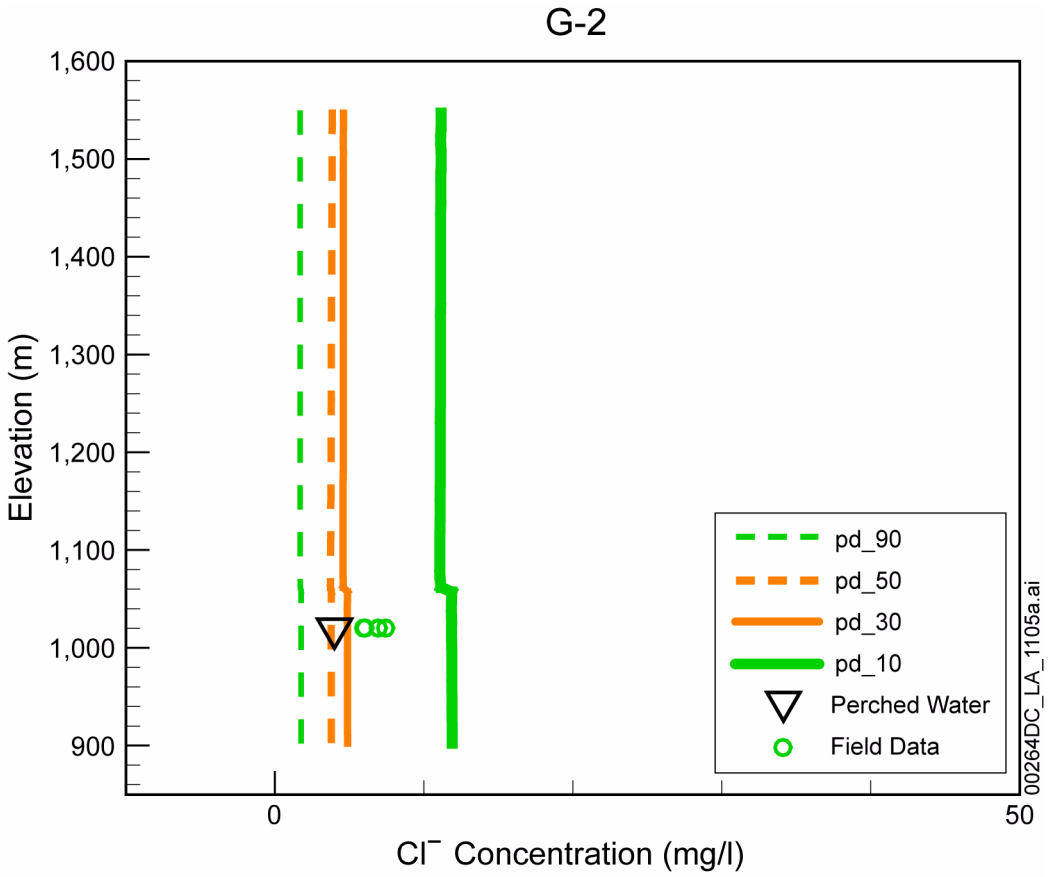

Figure 2.3.2-26. Chloride Concentration (mg/L) Profiles at Borehole USW G-2 for Present-Day 10th, 30th, 50th, and 90th Percentile Infiltration Maps

Source: SNL 2007a, Figure 6.5-9.

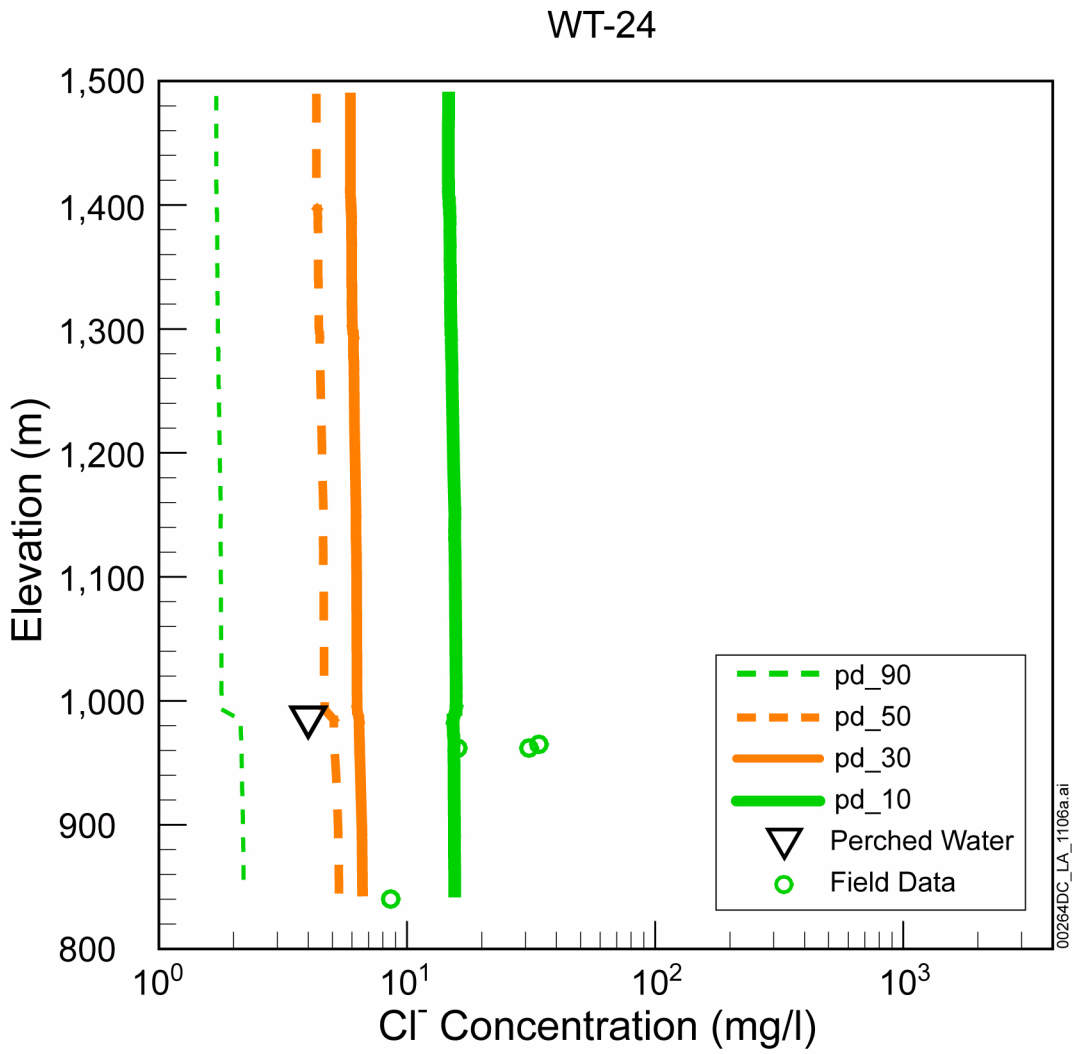

Figure 2.3.2-27. Chloride Concentration (mg/L) Profiles at Borehole USW WT-24 for Present-Day 10th, 30th, 50th, and 90th Percentile Infiltration Maps

Source: SNL 2007a, Figure 6.5-10.

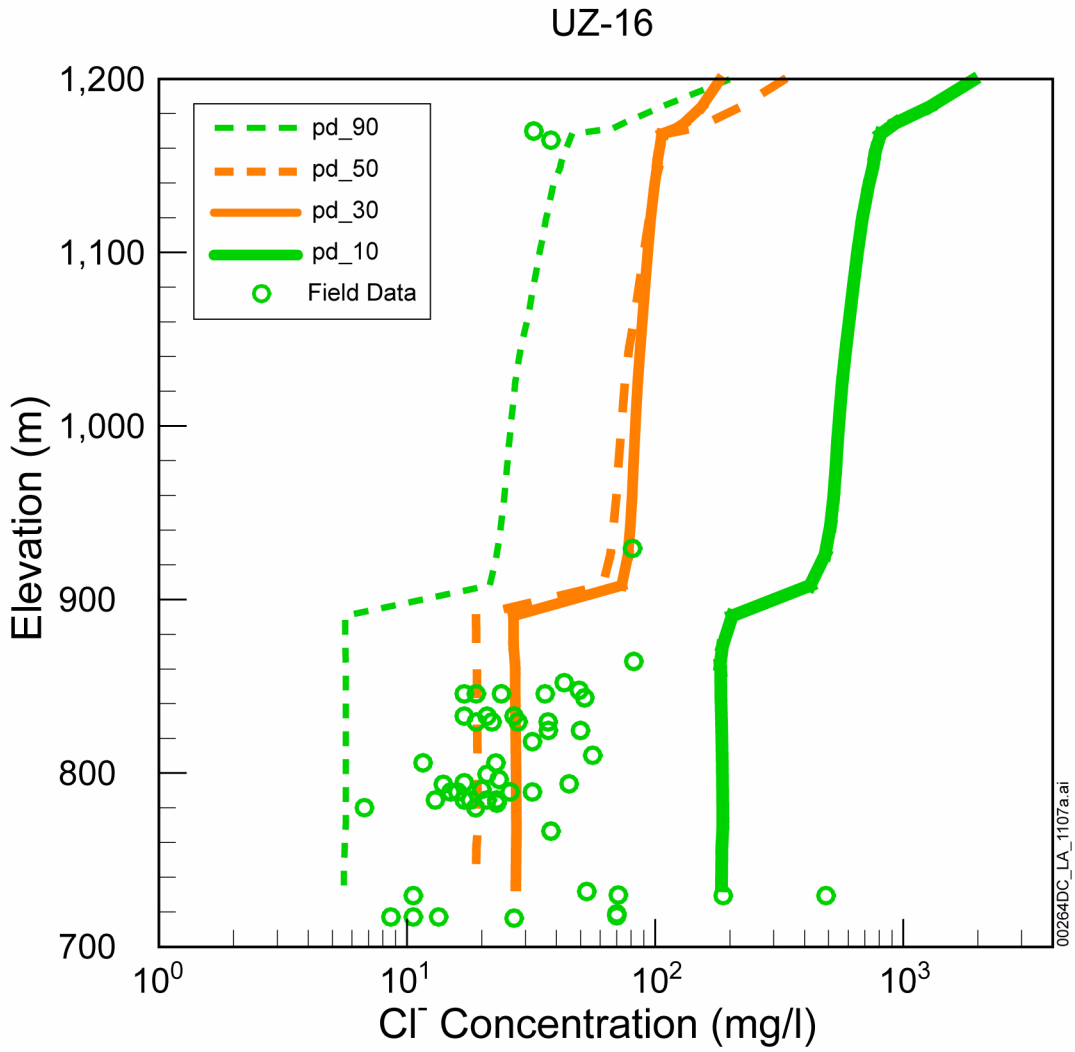

Figure 2.3.2-28. Chloride Concentration (mg/L) Profiles at Borehole USW UZ-16 for Present-Day 10th, 30th, 50th, and 90th Percentile Infiltration Maps

Source: SNL 2007a, Figure 6.5-11.

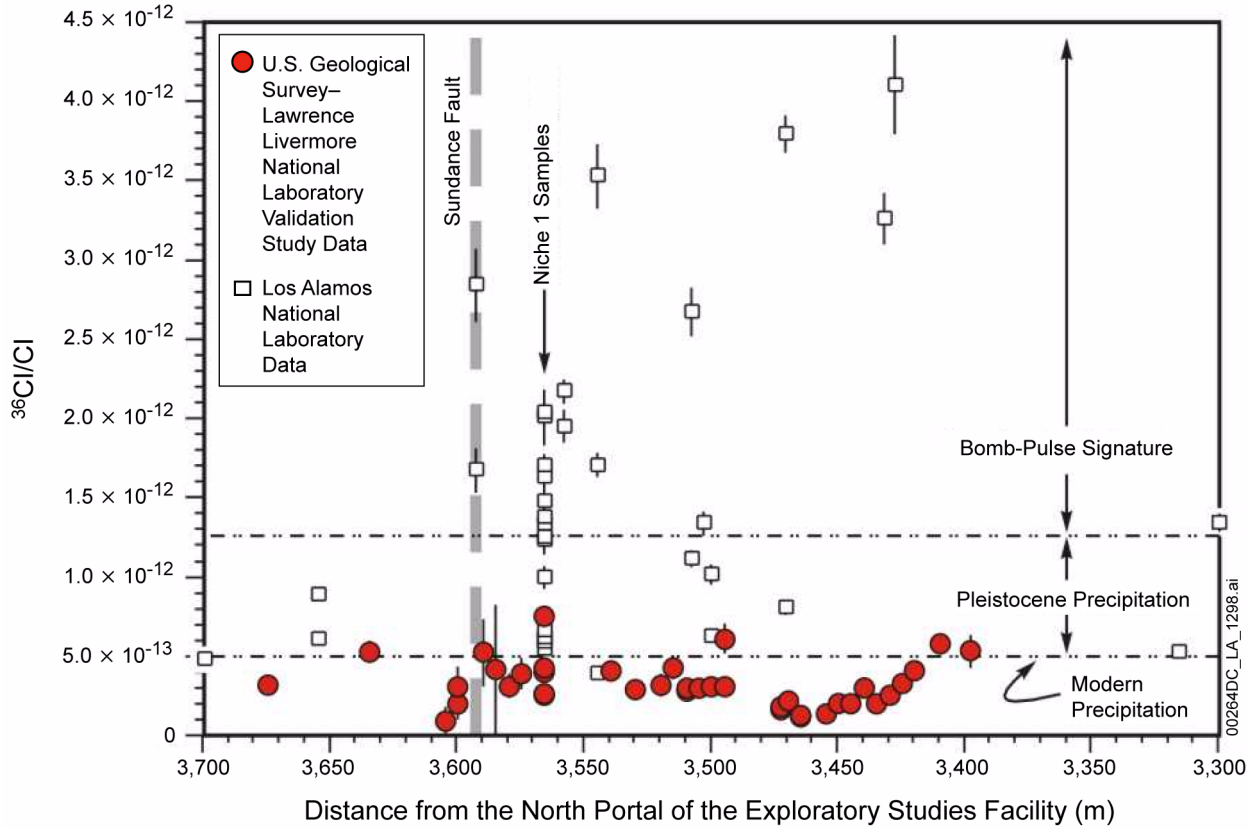

Figure 2.3.2-29. $^{36}Cl/Cl$ Ratio Plotted against Sample Location in the Exploratory Studies Facility

NOTE: Although the main trace of the Sundance Fault (shaded broad dashes) is exposed at a distance of 3,593 m from the ESF North Portal, the entire zone between about 3,400 and 3,650 m is pervasively fractured. For each ratio, the range of analytical errors (2σ) is shown as a vertical line if it is larger than the size of the symbol.

Source: BSC 2004i, Figure 6-195.

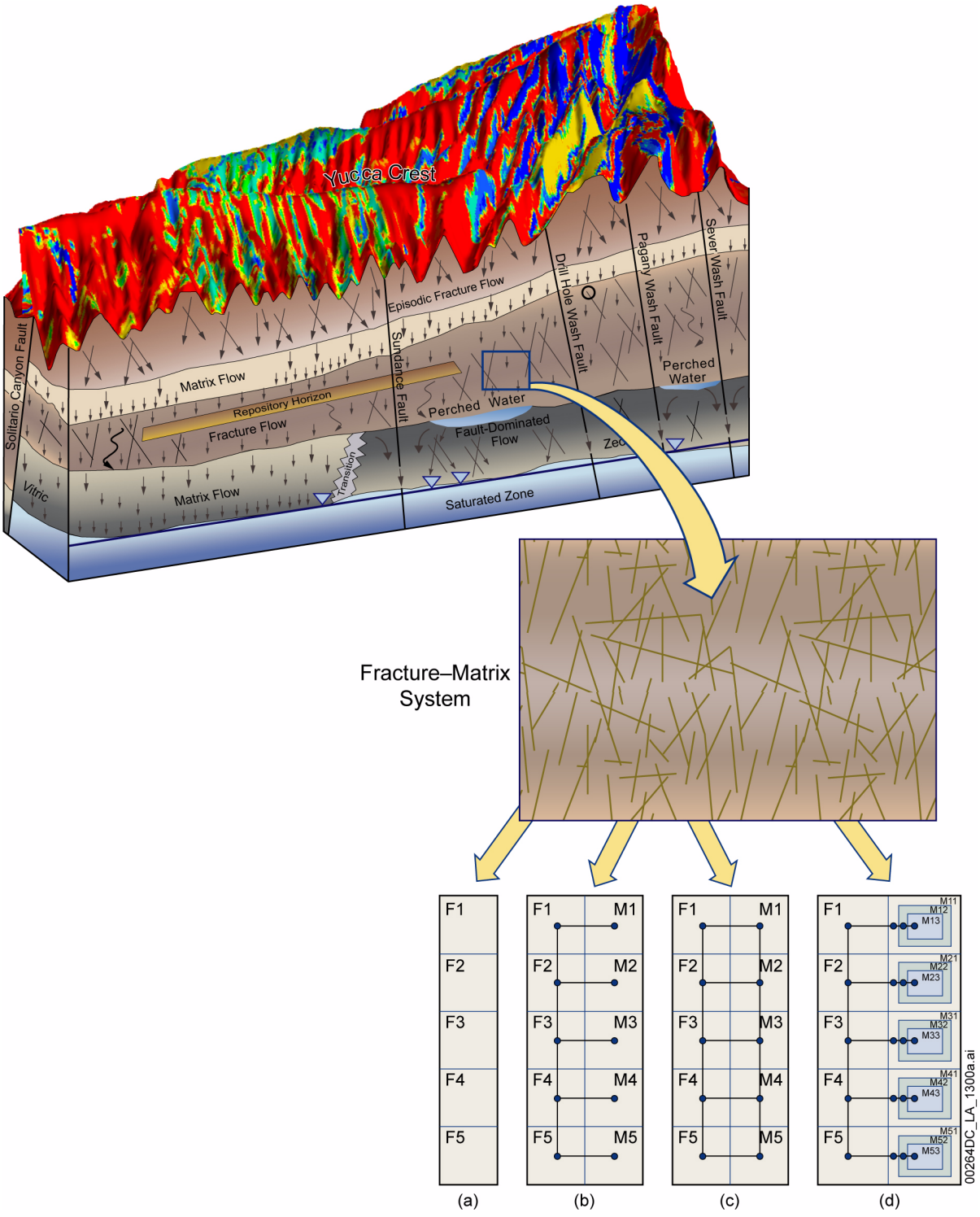

Figure 2.3.2-30. Schematic Fracture–Matrix System and Flow Conceptualization

NOTE: Effective-continuum model (a), dual-porosity with one matrix gridblock (b), dual-permeability with one matrix gridblock per fracture gridblock (c), and multiple-interacting-continua model with three matrix gridblocks per fracture gridblock (d).

Source: BSC 2004f, Figures 6-3 and 6-7.

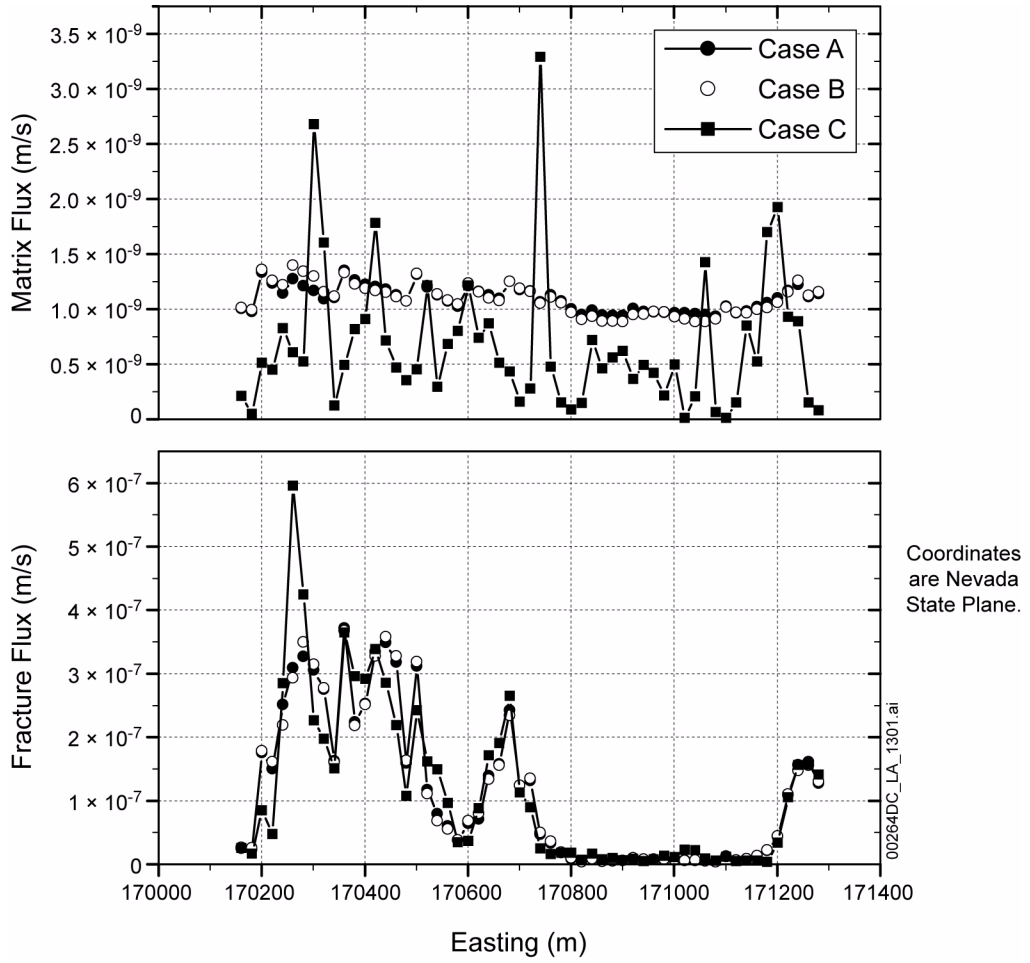

Figure 2.3.2-31. Comparison of Simulated Matrix and Fracture Flux at the Repository Horizon for Three Alternative Heterogeneous Property Cases

NOTE: Case A used mean rock properties for all layers. Case B used stochastic fracture permeability for all layers. Case C used stochastic fracture permeability, matrix permeability, and matrix van Genuchten α parameter for all layers.

Source: BSC 2004f, Figure 6-10.

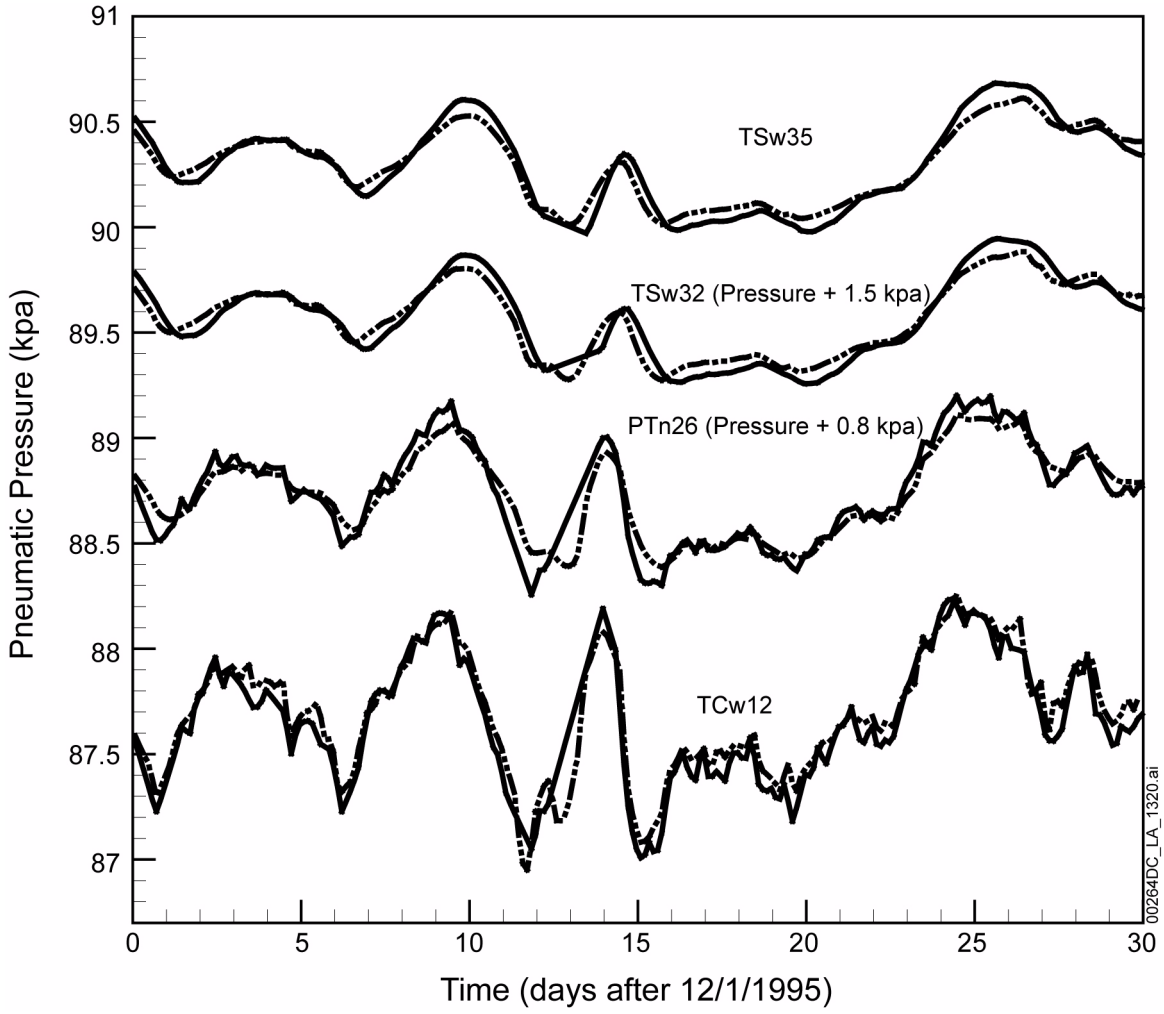

Figure 2.3.2-32. Pneumatic Pressure Matches at USW SD-12 for the One-Dimensional, Mountain-Scale, Calibrated Parameter Set for the 10th Percentile Infiltration Map

NOTE: Solid lines correspond to the interpolated raw data and dashed lines to simulated results.

Source: SNL 2007c, Figure 6-9.

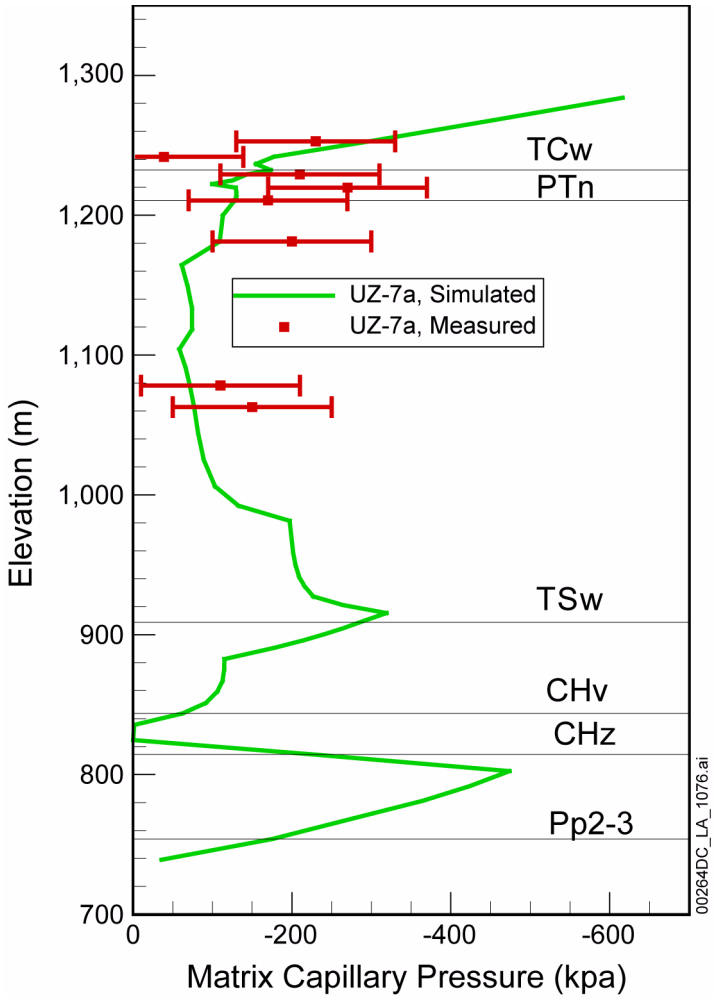

Figure 2.3.2-33. Water-Potential Matches at USW UZ-7a Used in the Two-Dimensional Calibrated Fault Parameter Set for the 10th Percentile Infiltration Map

Source: SNL 2007c, Figure 6-11.

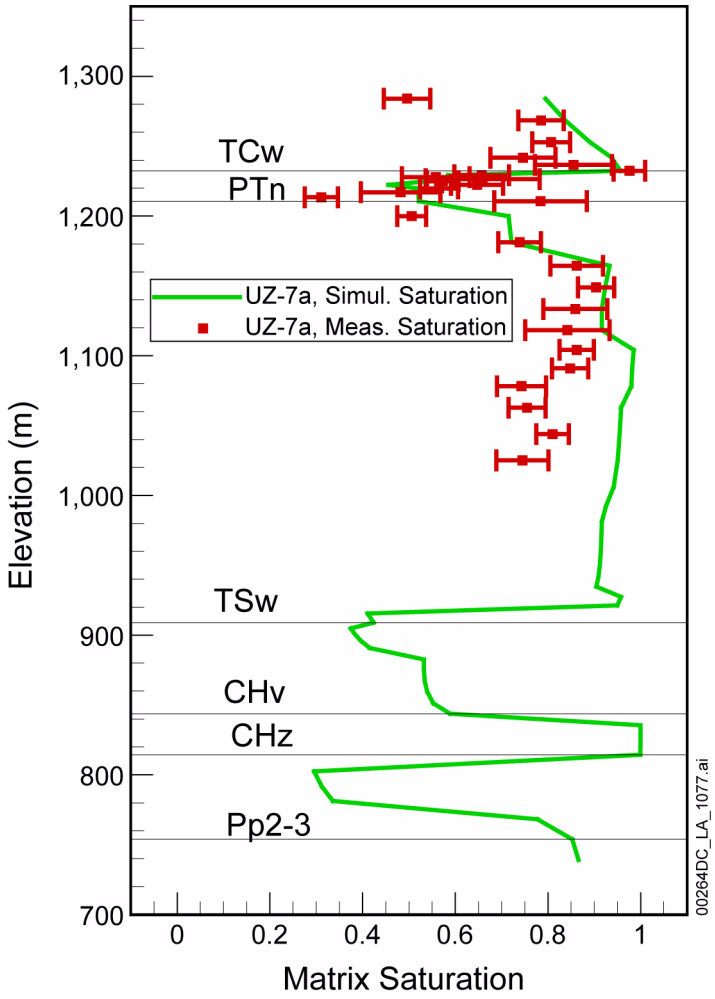

Figure 2.3.2-34. Saturation Matches at USW UZ-7a Used in the Two-Dimensional Calibrated Fault Parameter Set for the 10th Percentile Infiltration Map

Source: SNL 2007c, Figure 6-10.

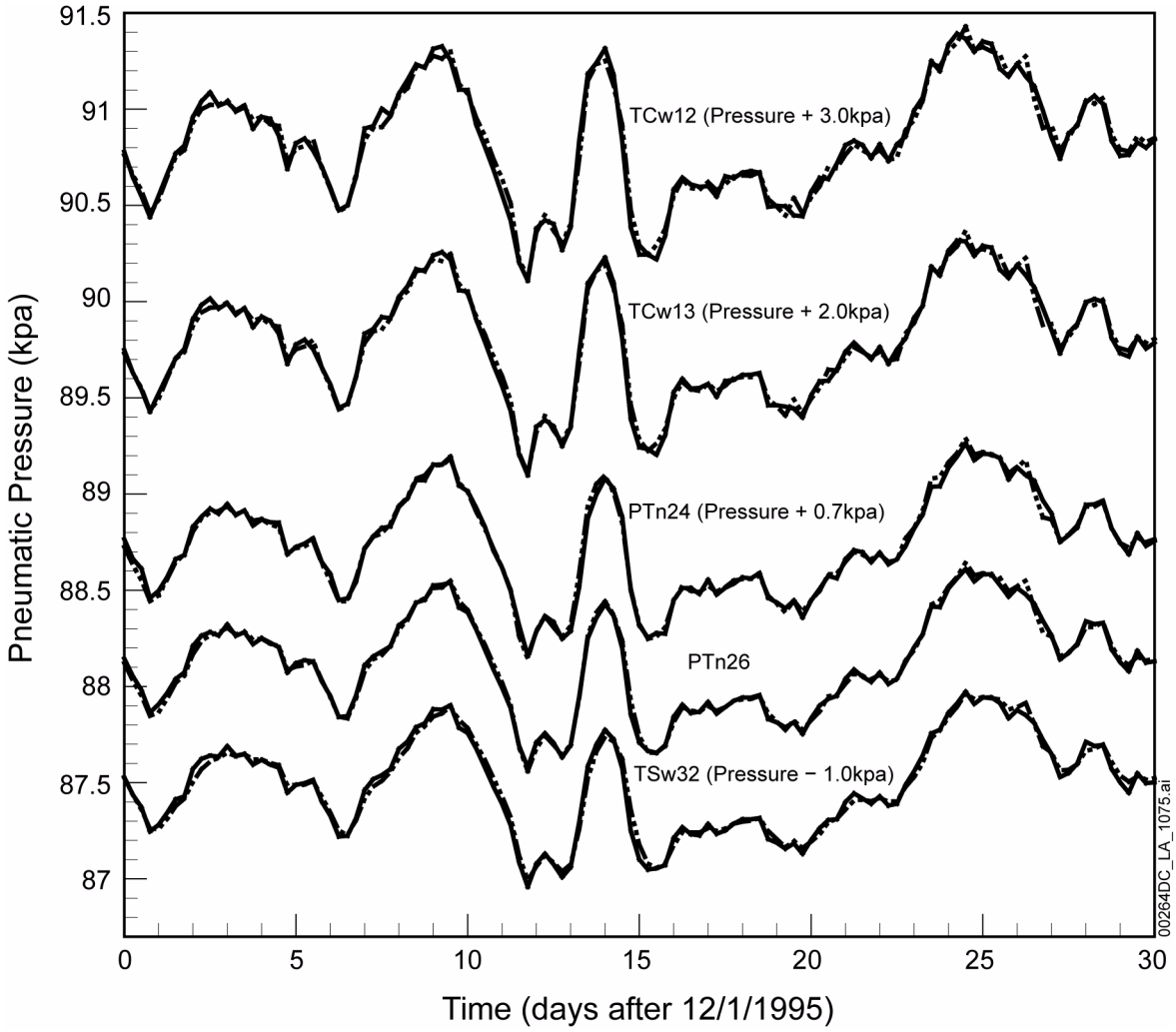

Figure 2.3.2-35. Pneumatic Pressure Matches at USW UZ-7a Used in the Two-Dimensional Calibrated Fault Parameter Set for the 10th Percentile Infiltration Map

NOTE: Solid lines correspond to the interpolated raw data and dashed lines to simulated results.

Source: SNL 2007c, Figure 6-12.

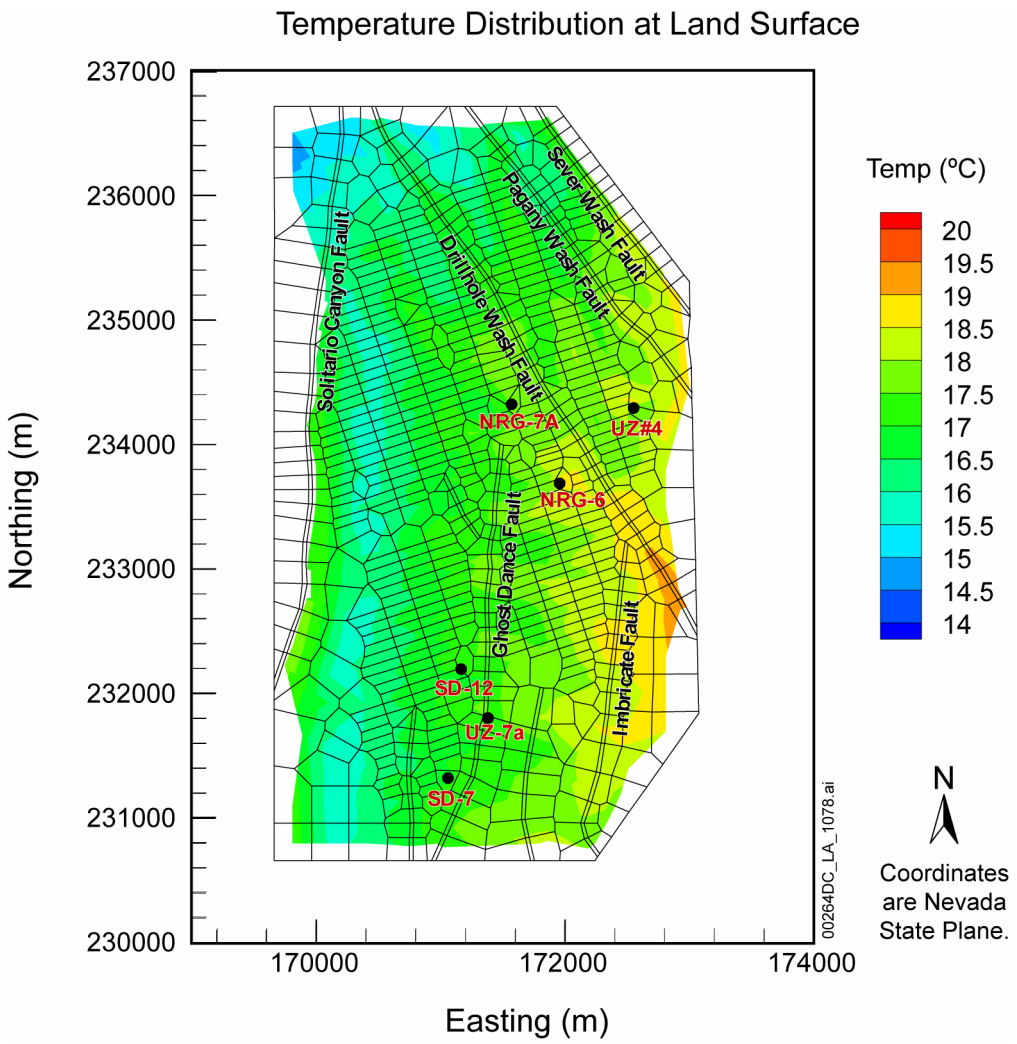

Figure 2.3.2-36. Temperature Distributions at the Mountain Surface, the Top Model Boundary for Present-Day Infiltration

Source: SNL 2007a, Figure 6.3-8.

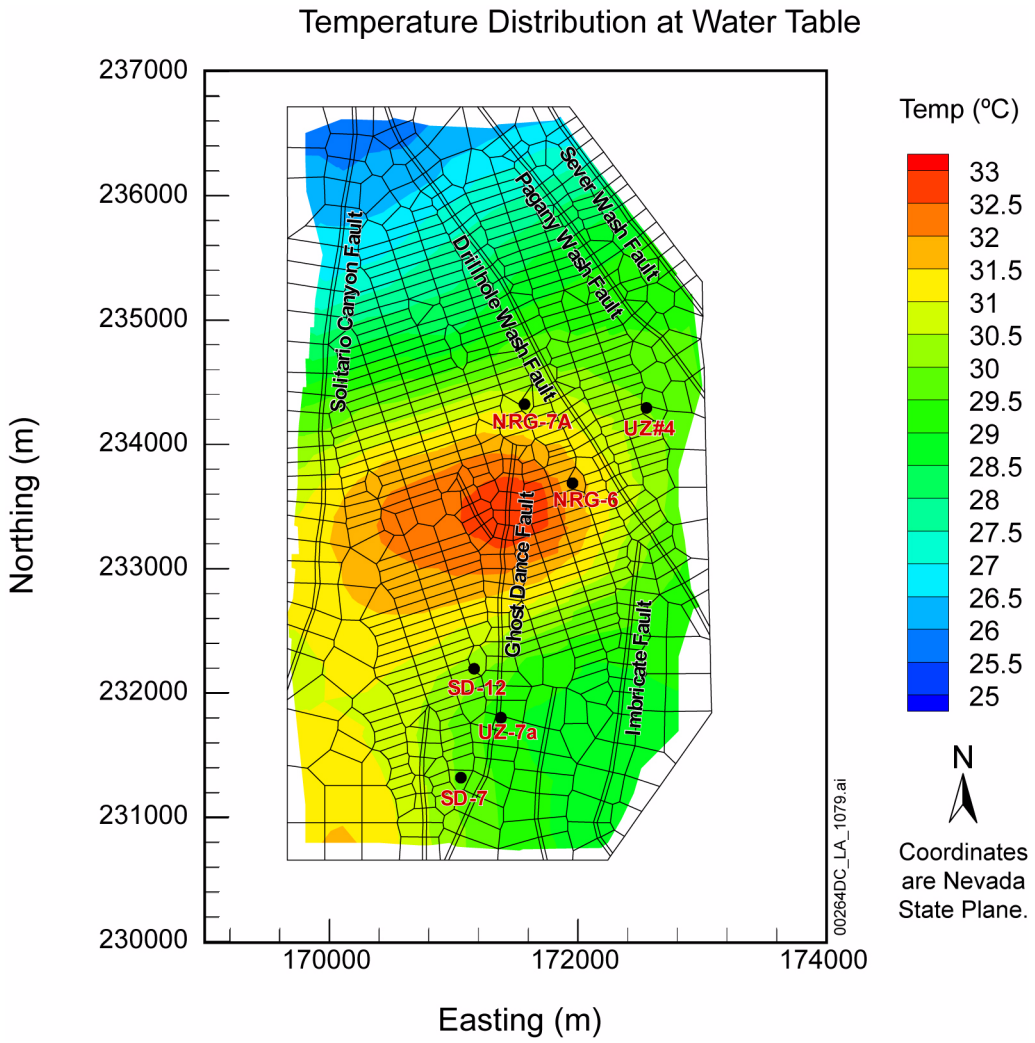

Figure 2.3.2-37. Ambient Temperature Distributions at the Water Table for Present-Day Infiltration

Source: SNL 2007a, Figure 6.3-7.

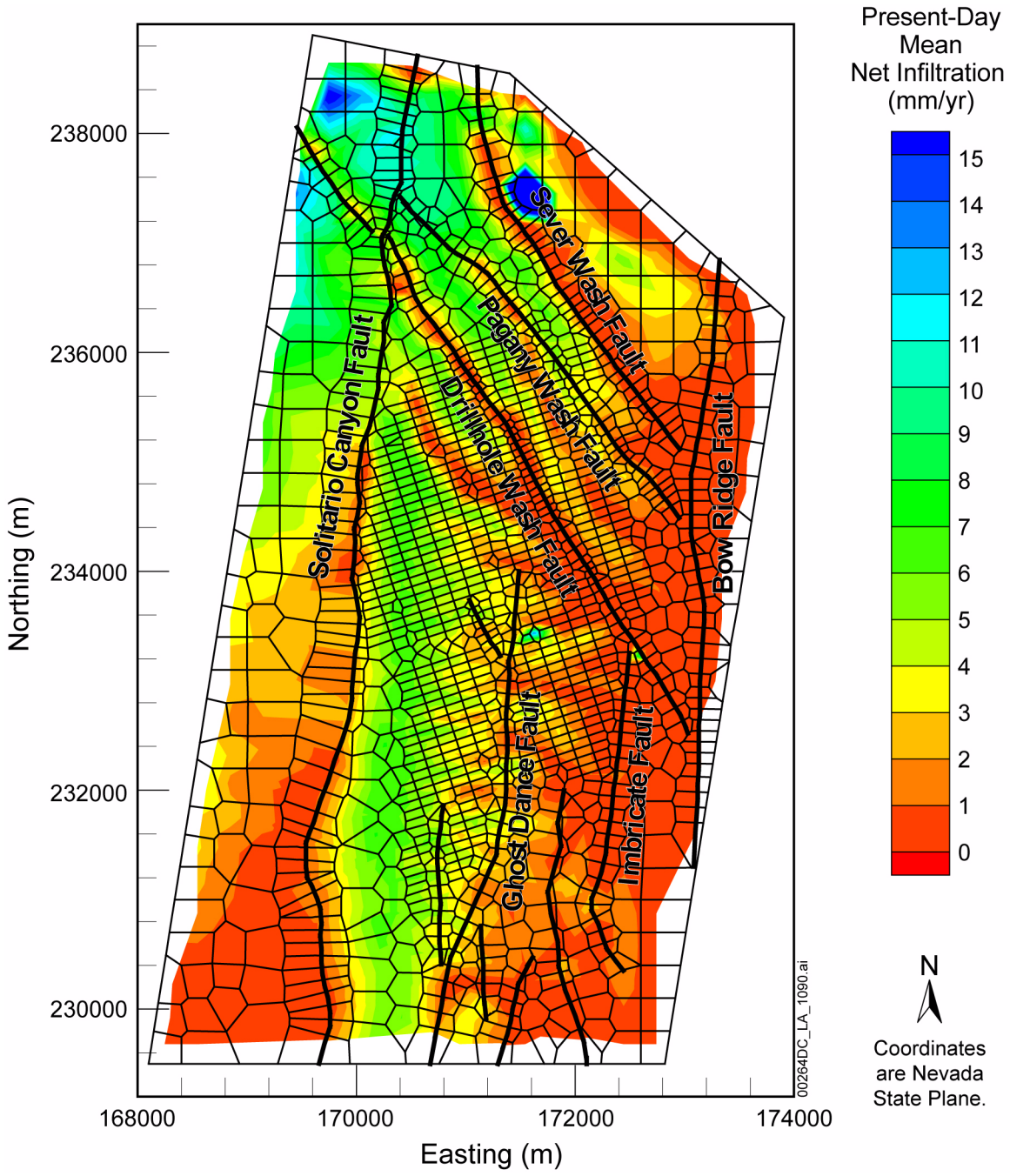

Figure 2.3.2-38. Plan View of Net Infiltration Distributed over the Three-Dimensional Site-Scale Unsaturated Zone Flow Model Grid for the Present-Day 10th Percentile Infiltration Map

Source: SNL 2007a, Figure 6.1-2.

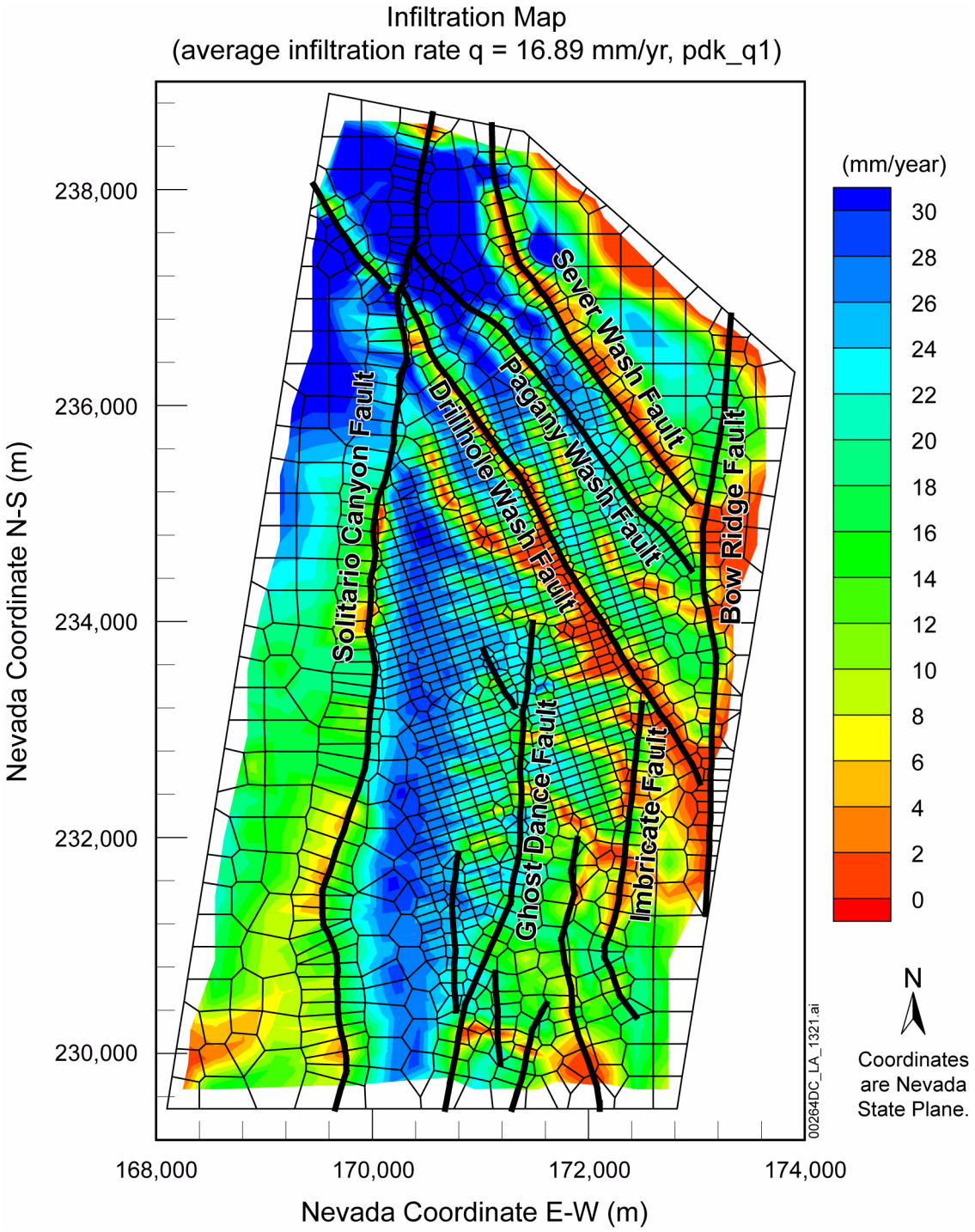

Figure 2.3.2-39. Plan View of Net Infiltration Distribution over the Three-Dimensional Unsaturated Zone TSPA Model Grid for the Post-10,000-year Period Climate, 31st Percentile Infiltration Scenario

Source: SNL 2007a, Figure 6.1-5.

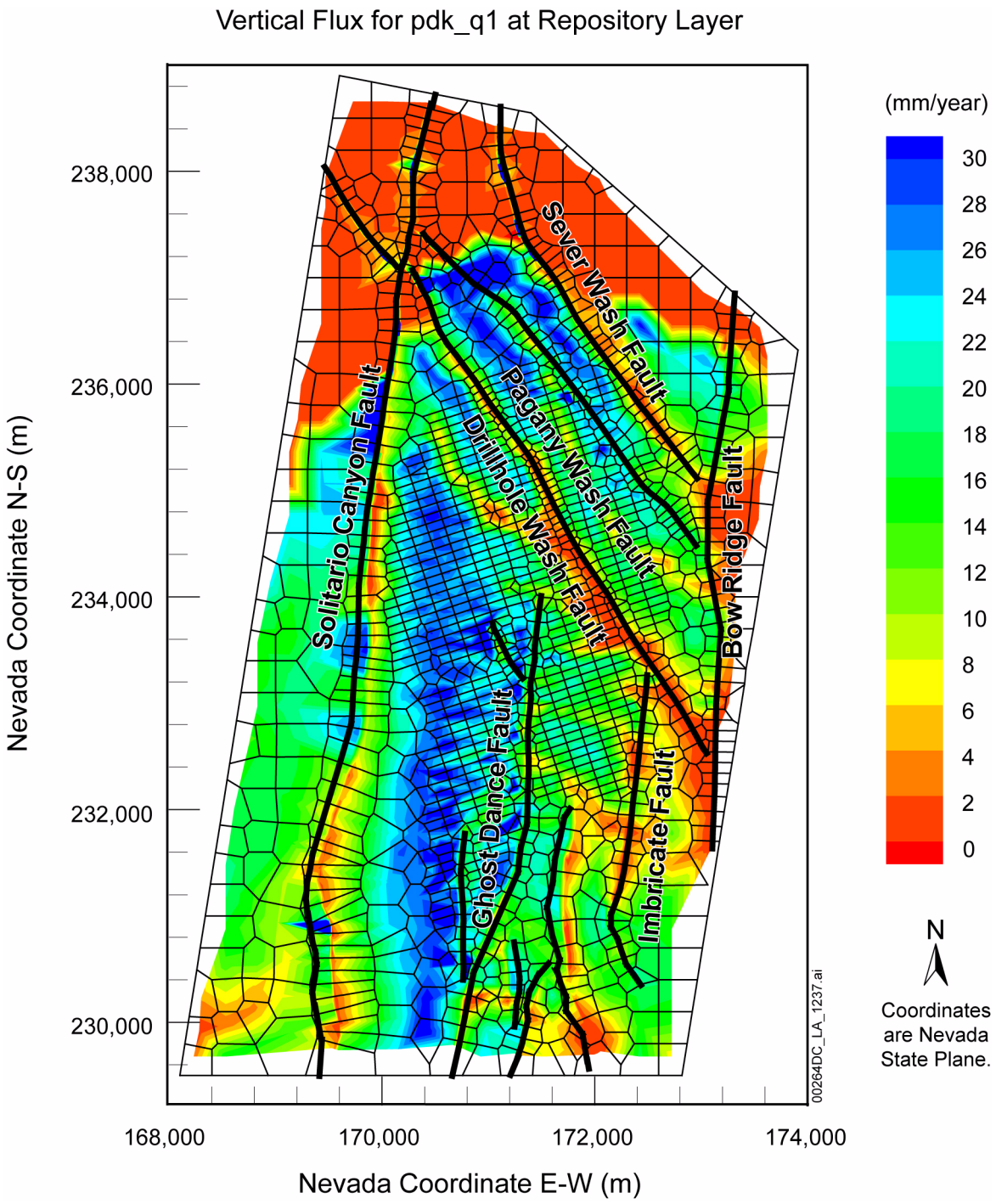

Figure 2.3.2-40. Simulated Percolation Fluxes at the Repository Horizon under the Post-10,000-Year, 31st Percentile Infiltration Scenario

Source: SNL 2007a, Figure 6.6-4.

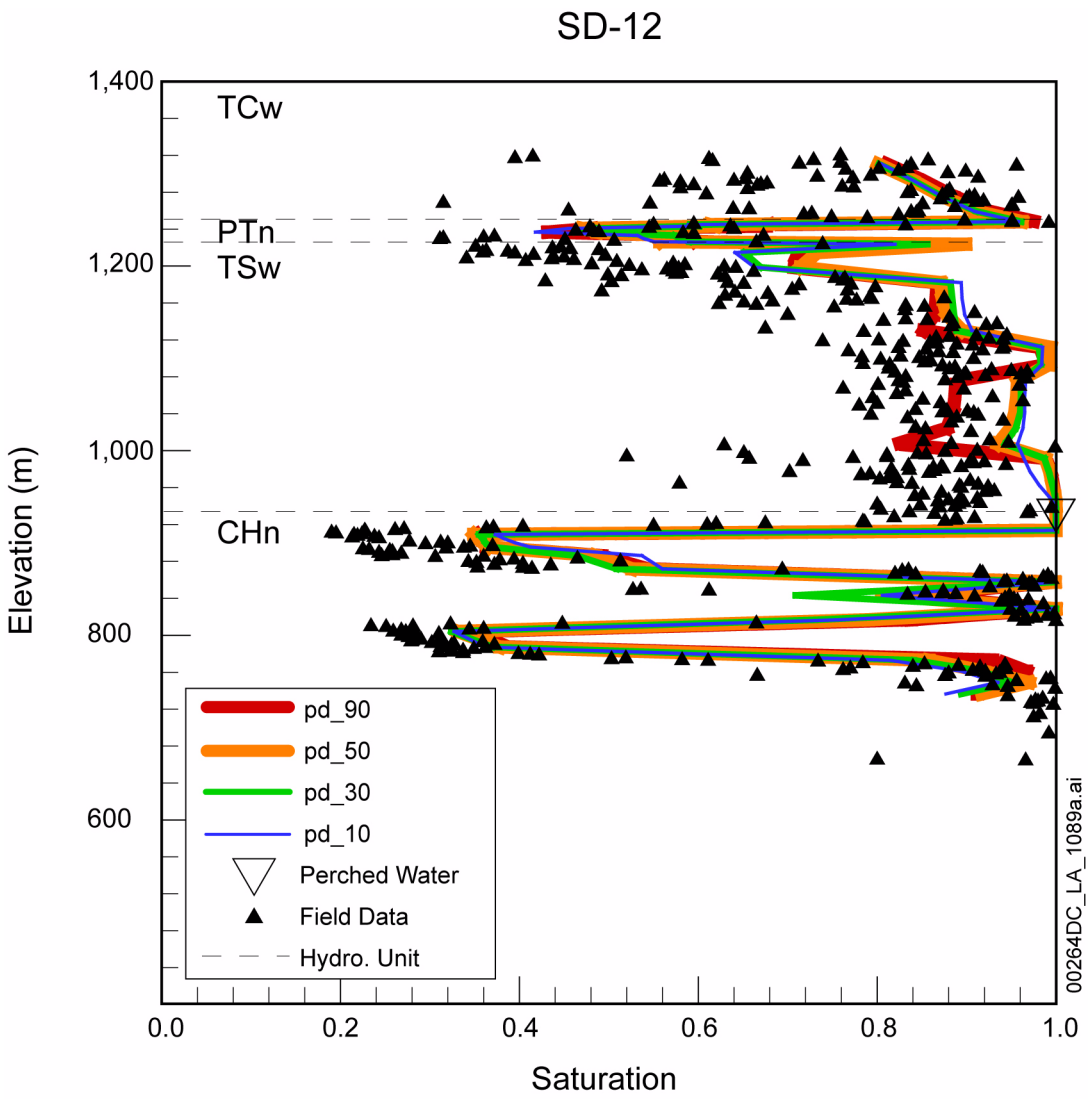

Figure 2.3.2-41. Comparison of the Simulated to the Observed Matrix Liquid Saturations and Perched-Water Elevations for Borehole USW SD-12, Using the Results of the Simulations with Four Present-Day Infiltration Rates

Source: SNL 2007a, Figure 6.2-3.

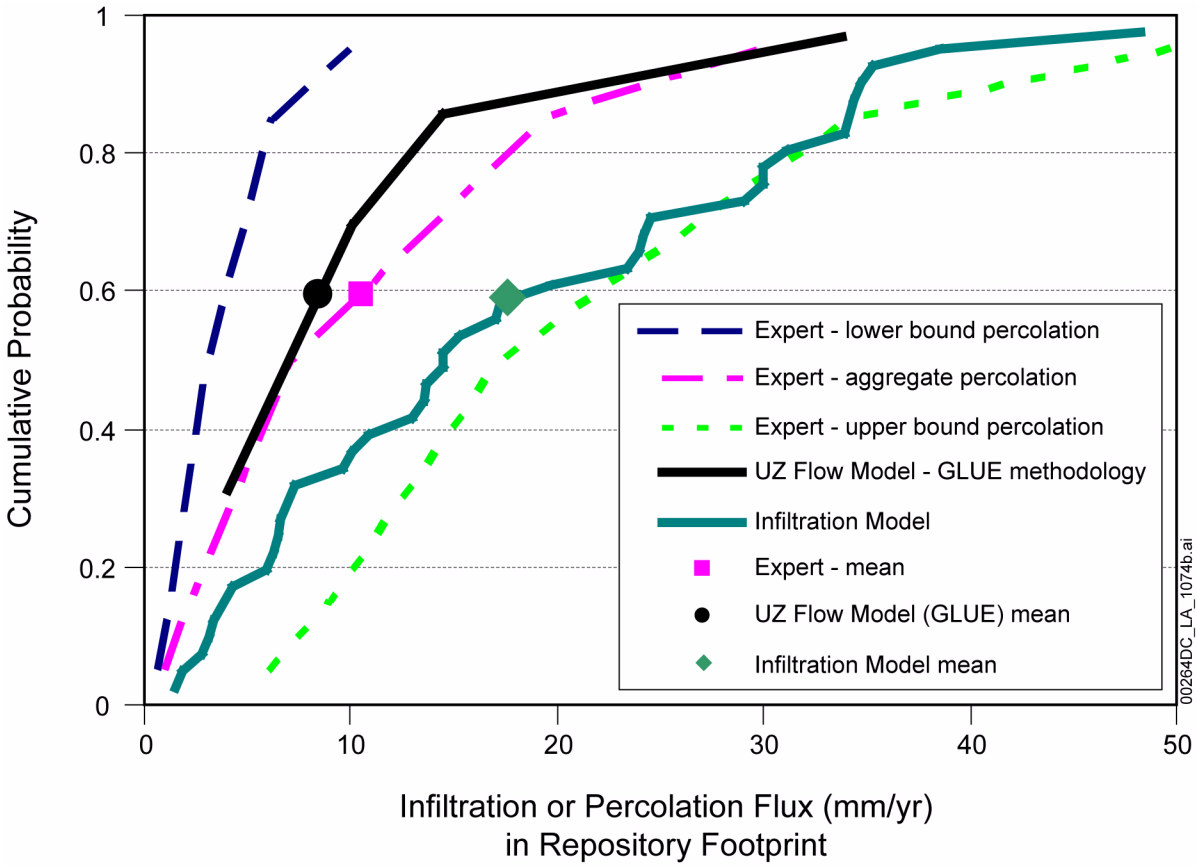

Figure 2.3.2-42. Comparison of Unsaturated Zone Flow Model Results using GLUE Methodology and Infiltration Model Results for Infiltration in the Repository Footprint with the Expert Elicitation Results for Percolation at the Repository

NOTE: Infiltration model results based on 2002 repository design footprint. See SNL 2008a, Section 1.
UZ = unsaturated zone.

Source: SNL 2007a, Figure 6.8-3[a].

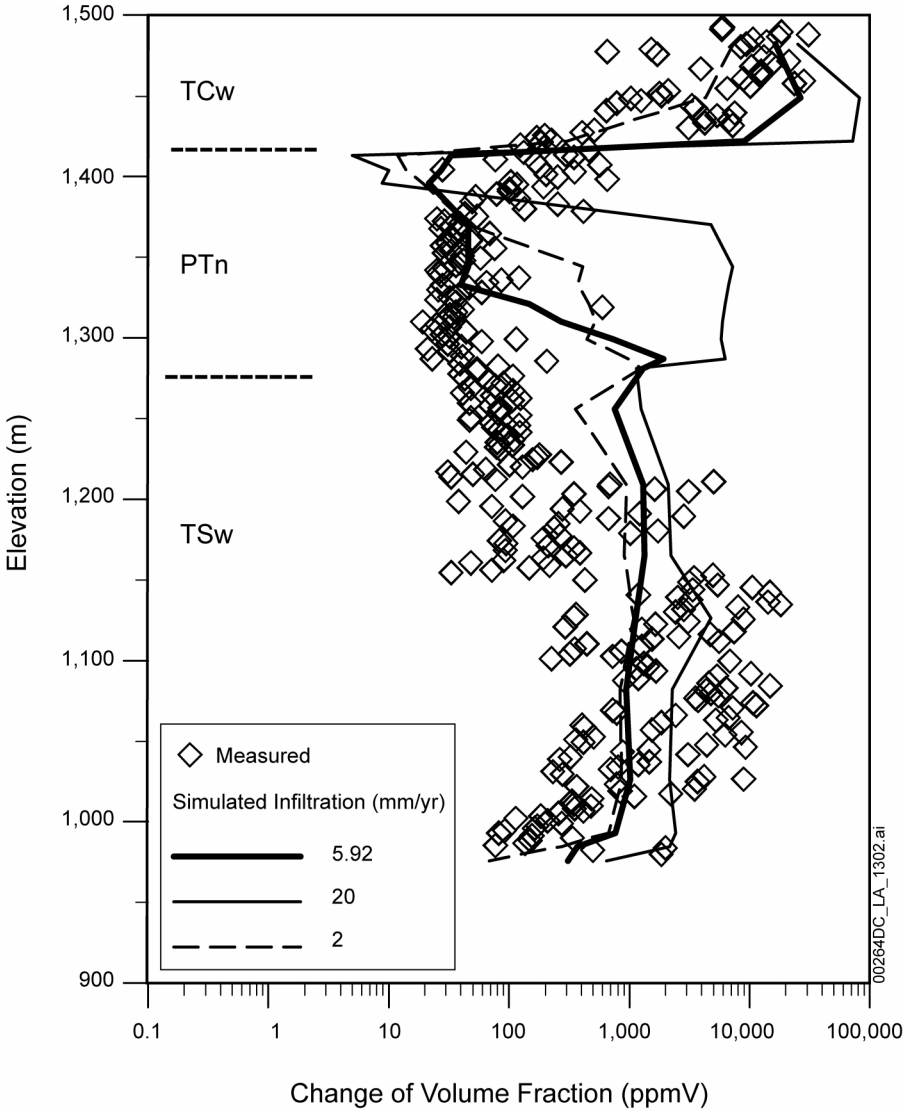

Figure 2.3.2-43. Comparison of Measured to Simulated Total (Fracture plus Matrix) Calcite Abundances in the USW WT-24 Column for Different Infiltration Rates

Source: SNL 2007a, Figure 7.7-3a.

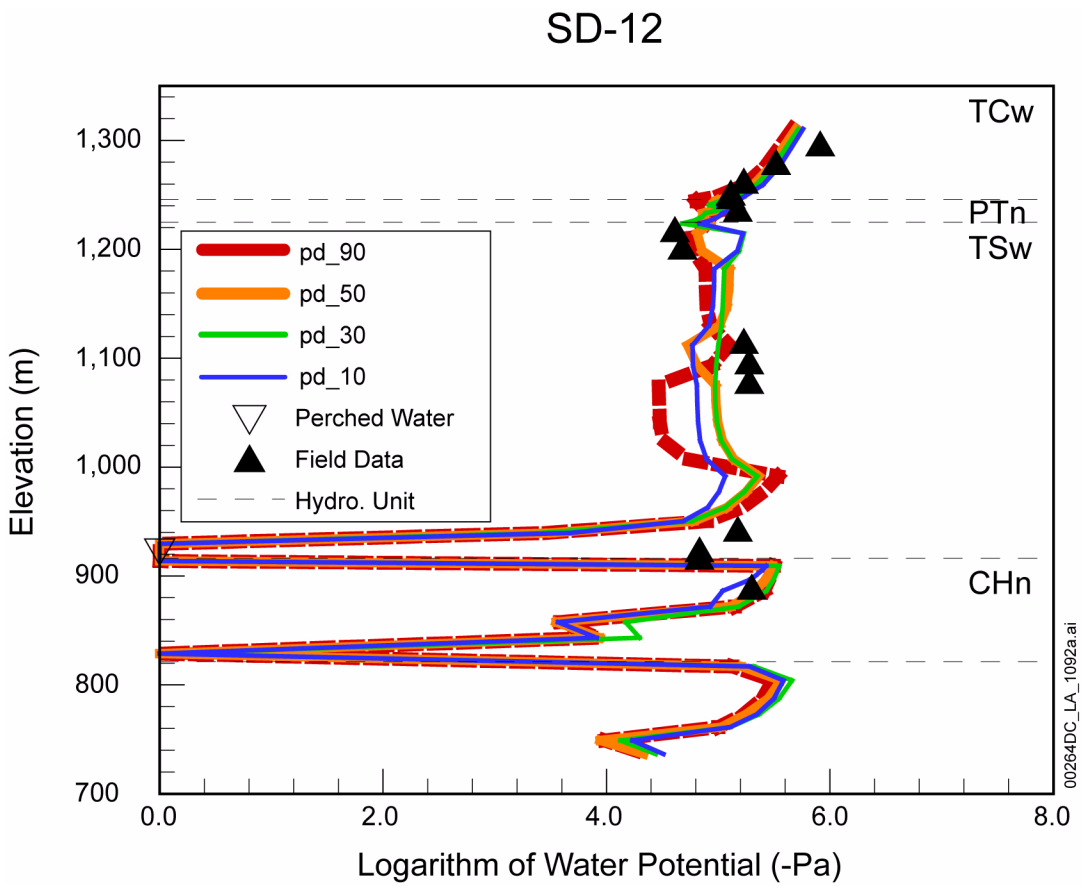

Figure 2.3.2-44. Comparison of the Simulated to the Averaged Observed Water Potentials and Perched-Water Elevations for Borehole USW SD-12, Using the Results of the Simulations with Four Present-Day Infiltration Rates

Source: SNL 2007a, Figure 6.2-4.

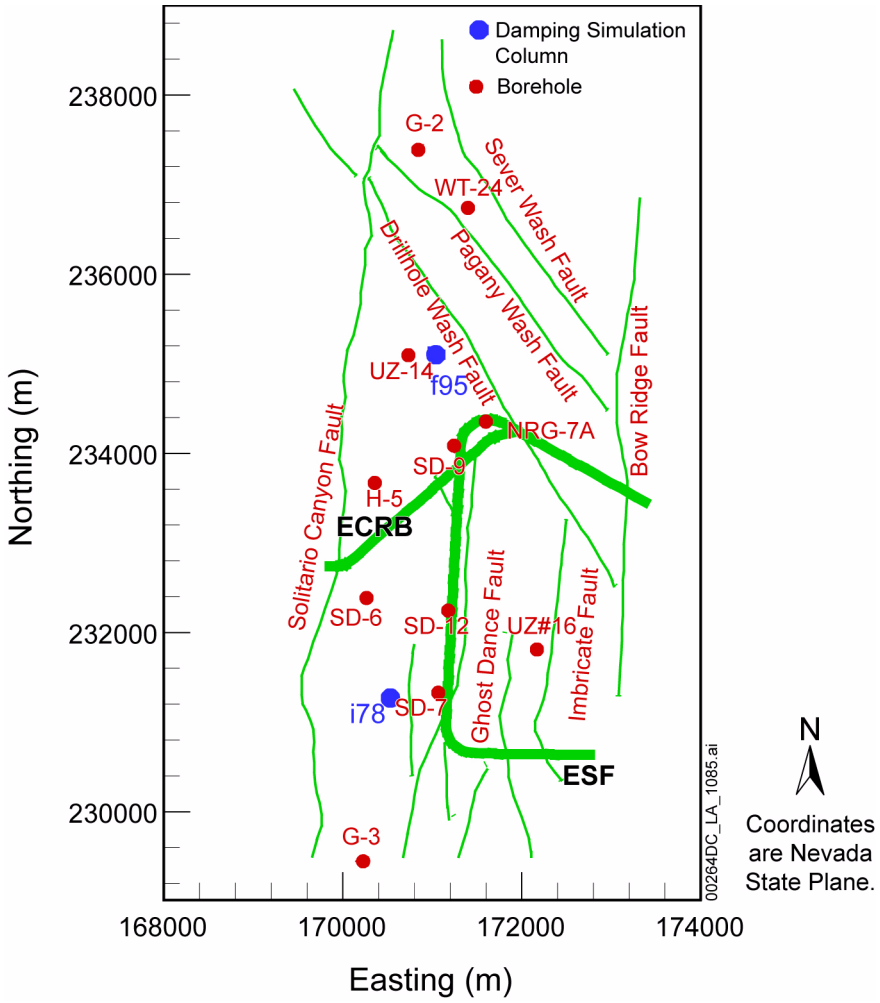

Figure 2.3.2-45. Location of the Columns for Damping Effect Simulation

Source: SNL 2007a, Figure 6.9-1.

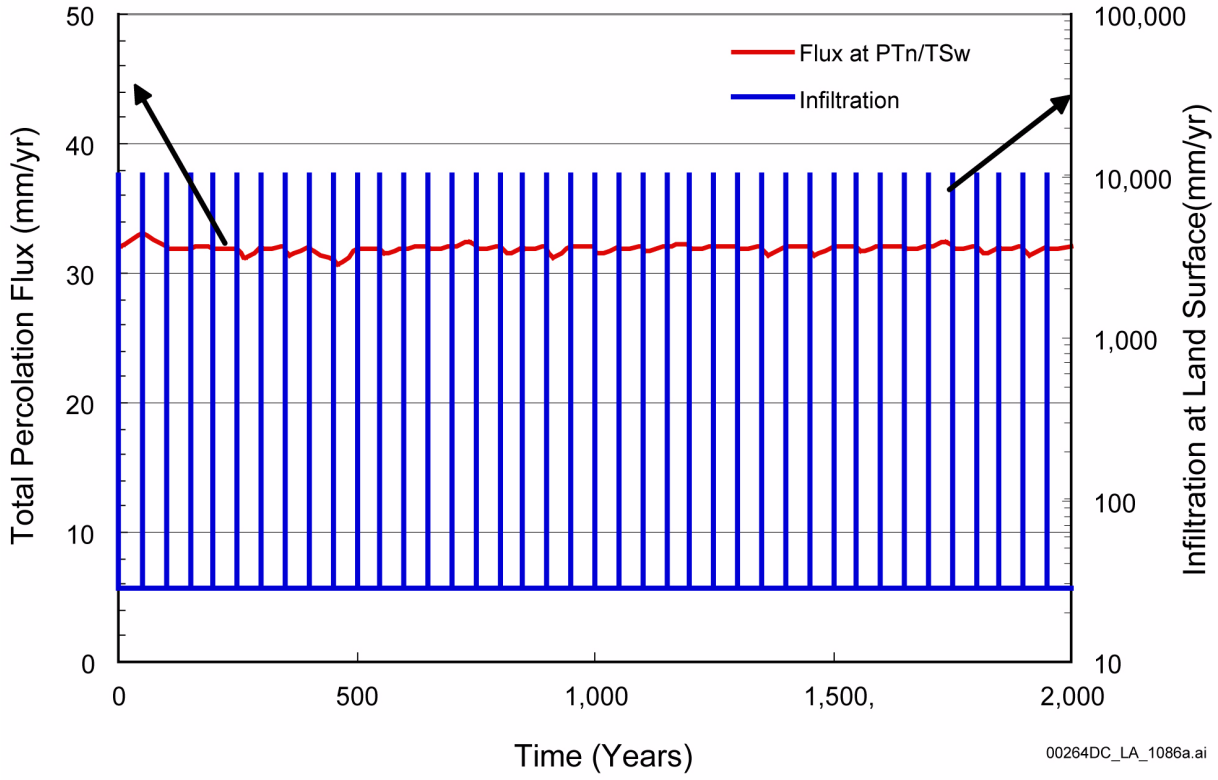

Figure 2.3.2-46. Infiltration Pulse and Simulated Variations in Total Percolation Fluxes Versus Times at the Bottom PTn Unit for Column f95 of the Unsaturated Zone Flow Model Grid

NOTE: The PTn unit has a thickness of 81 m at Column f95.

Source: SNL 2007a, Figure 6.9-2.

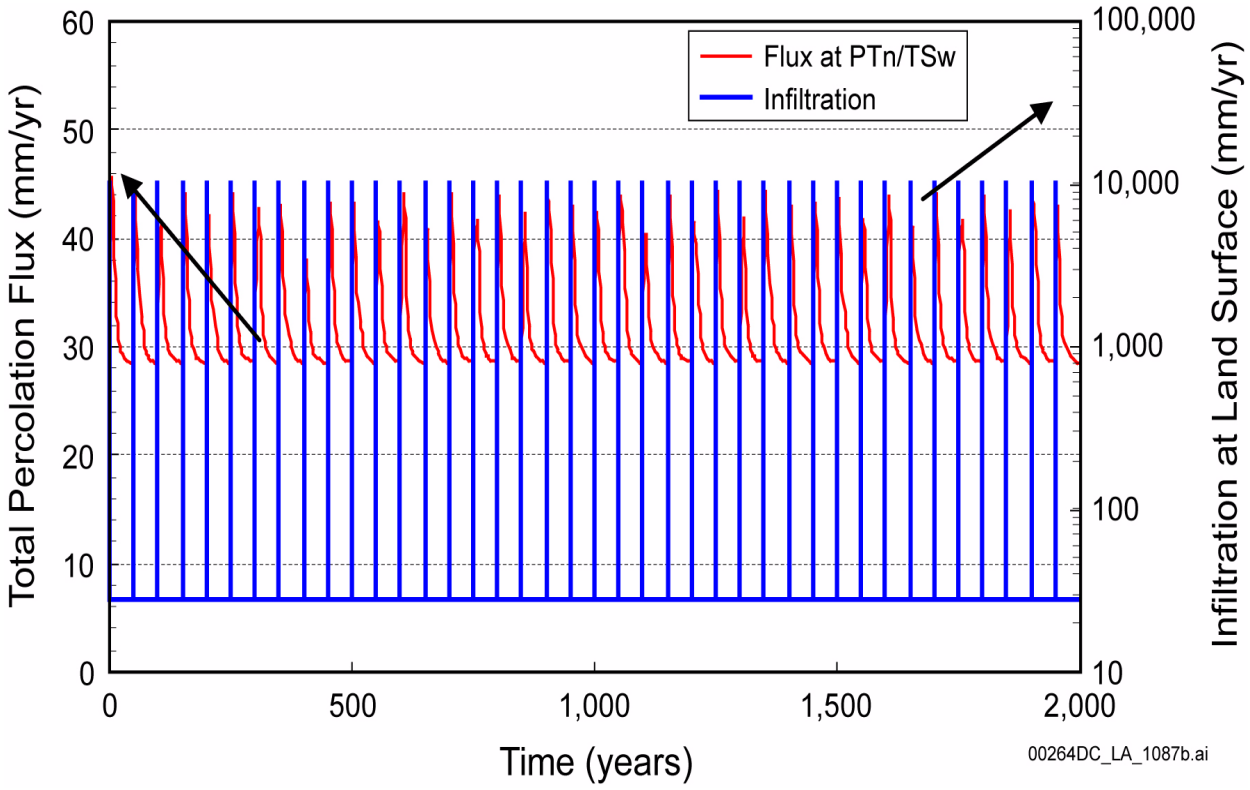

Figure 2.3.2-47. Infiltration Pulse and Simulated Variations in Total Percolation Fluxes Versus Times at the Bottom PTn Unit for Column i78 of the Unsaturated Zone Flow Model Grid

NOTE: The PTn unit has a thickness of 21 m at Column i78.

Source: SNL 2007a, Figure 6.9-3[a].

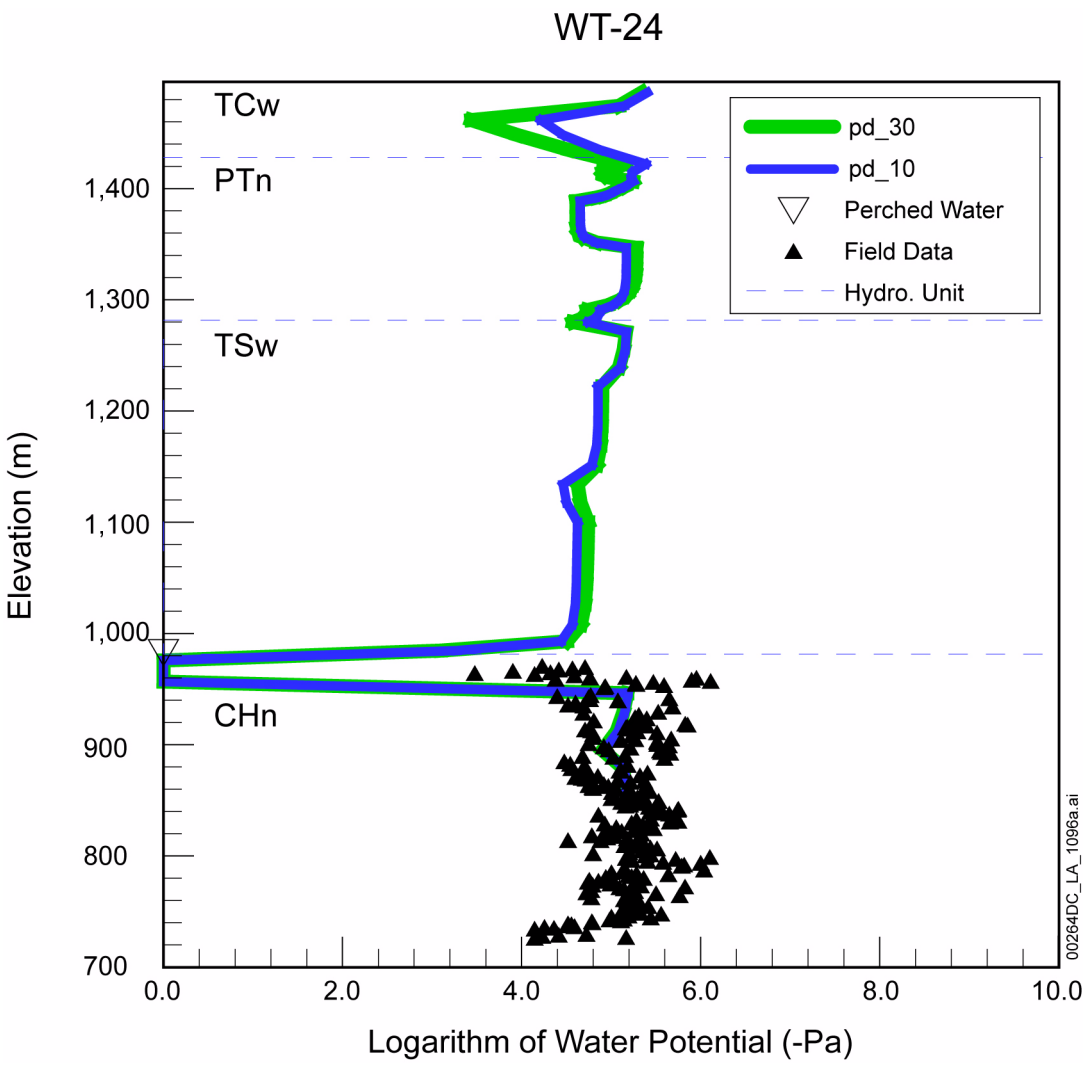

Figure 2.3.2-48. Comparison of Predicted to Measured Matrix Water Potentials and Perched-Water Elevations for Borehole USW WT-24, Using the Present-Day 10th and 30th Percentile Infiltration Maps

Source: SNL 2007a, Figure 7.3-1.

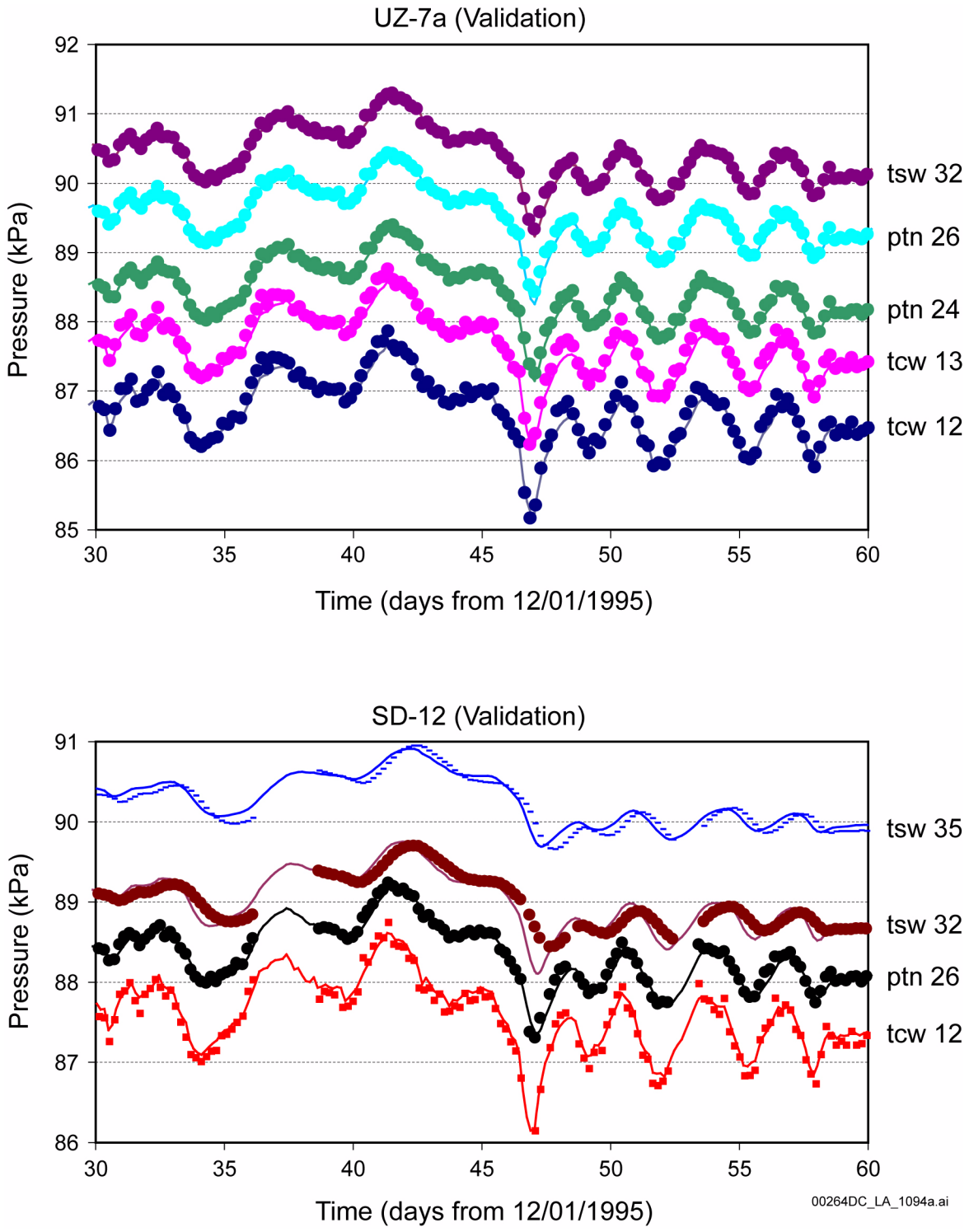

Figure 2.3.2-49. Comparison of Three-Dimensional Pneumatic Prediction (lines) to Observation Data (points) from Boreholes USW UZ-7a and USW SD-12 for the 10th Percentile Infiltration Map

Source: SNL 2007a, Figures 7.4-1 and 7.4-2.

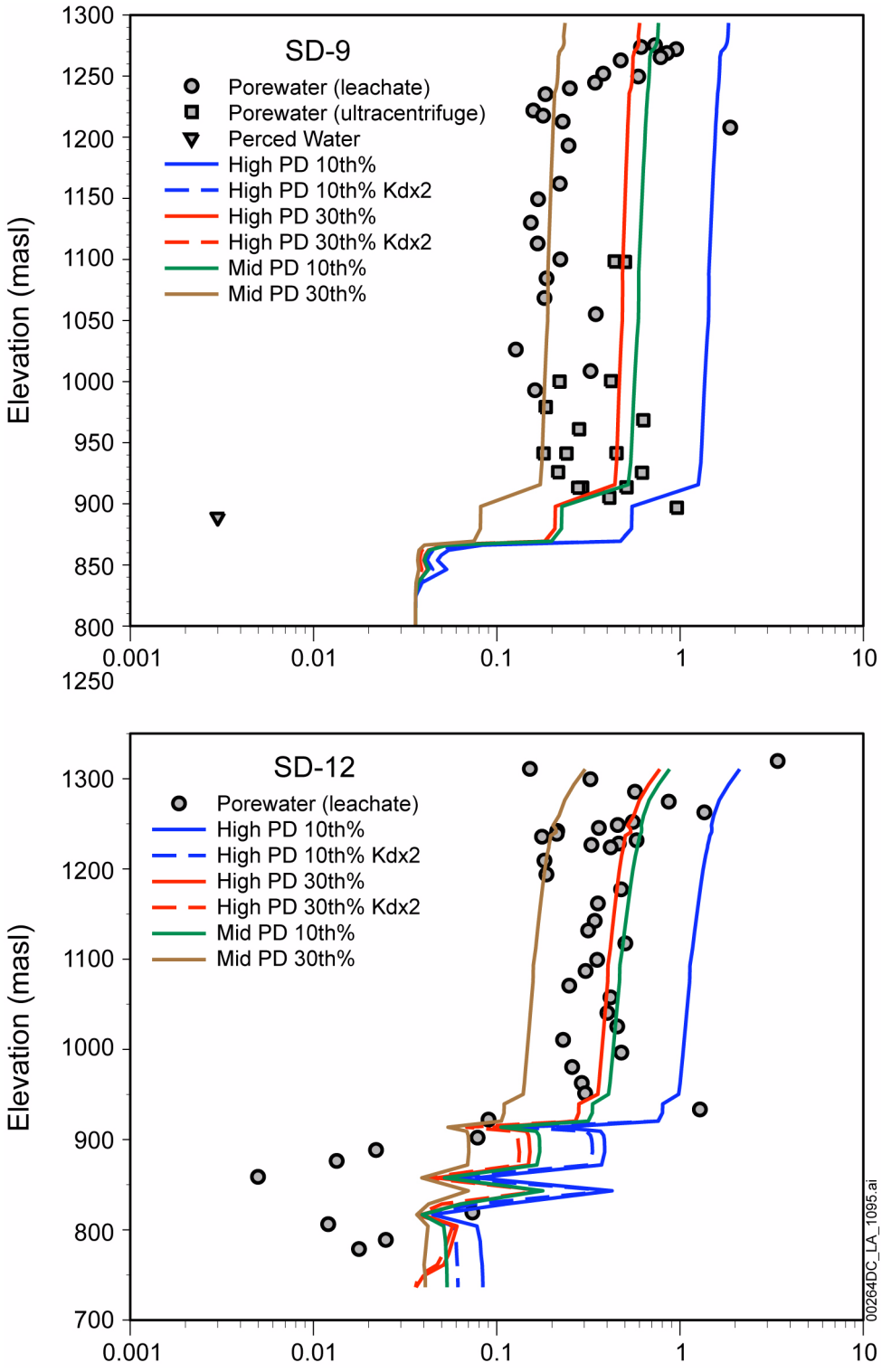

Figure 2.3.2-50. Comparison of Measured to Modeled Strontium Concentrations as a Function of Elevation for the Surface Based Boreholes USW SD-9 and USW SD-12

Source: SNL 2007a, Figure 7.6-1.

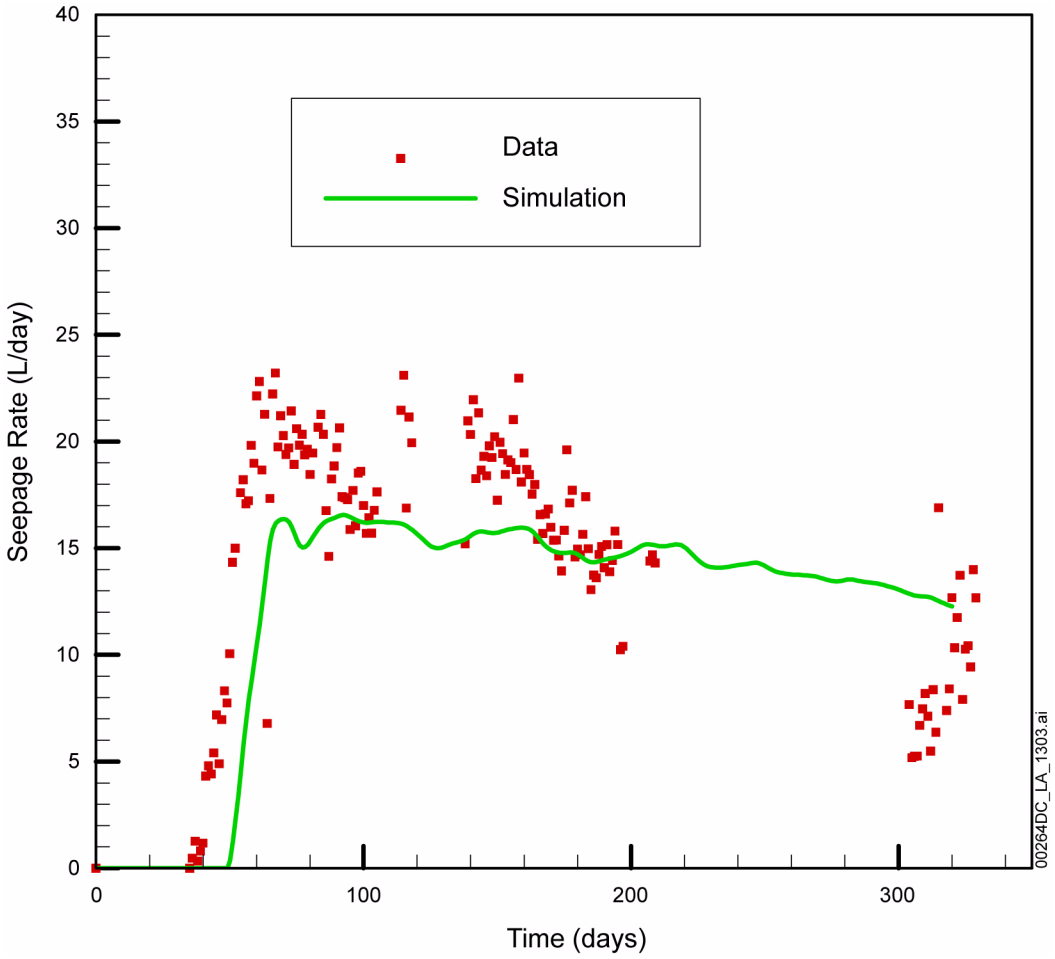

Figure 2.3.2-51. Comparison of Simulated Seepage Rates as a Function of Time to Field Observations Collected from Alcove 8–Niche 3 Tests

Source: SNL 2007a, Figure 7.8-8.

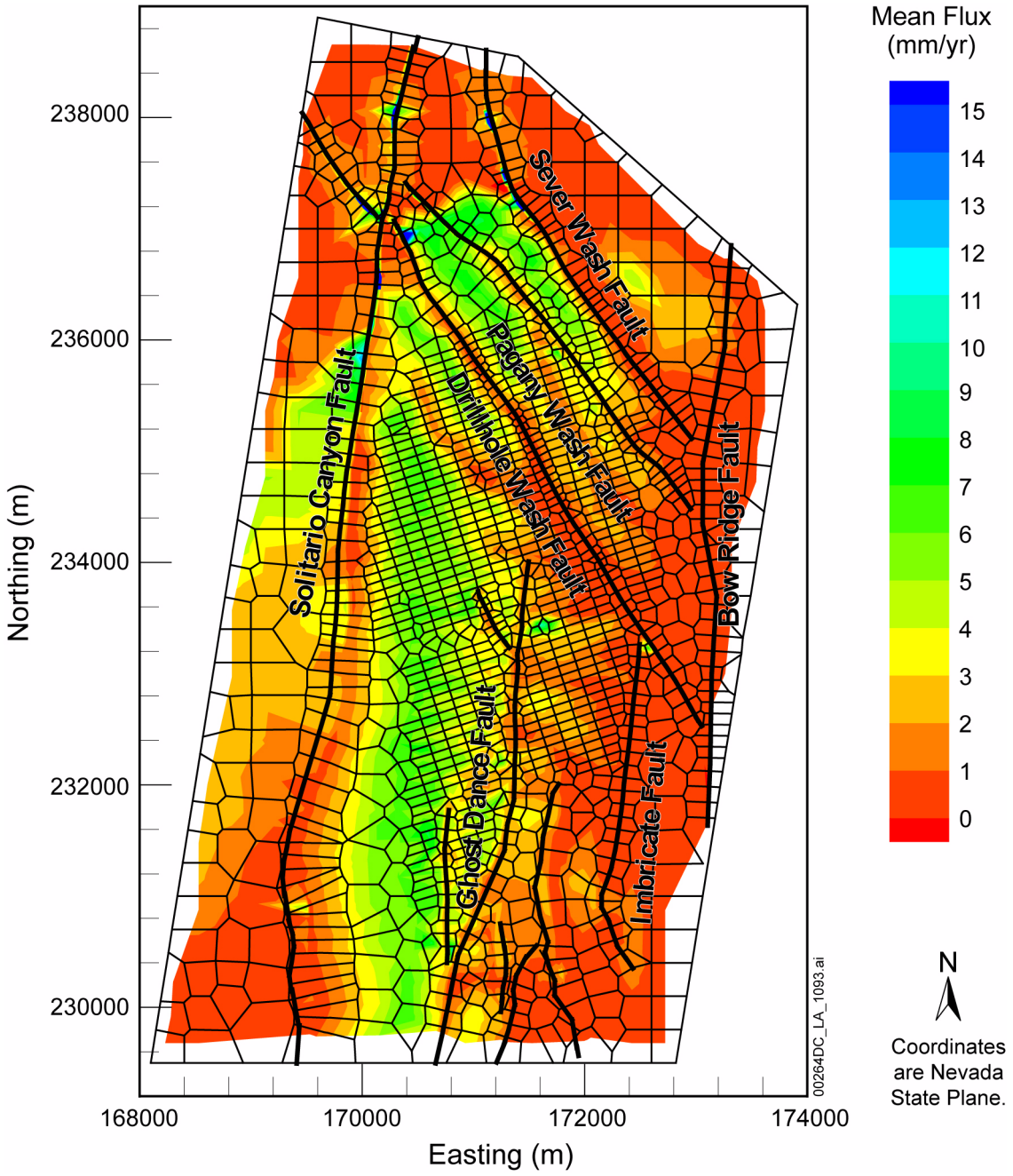

Figure 2.3.2-52. Simulated Percolation Fluxes at the Repository Horizon under the Present-Day, 10th Percentile Infiltration Map Using the Results of Simulation pd_10

Source: SNL 2007a, Figure 6.6-1.